

CHALMERS



Investigation of bus users' motion comfort due to wind and bridge motion excitations

Automotive Engineering Project TME180

Group D:

Albijon Blakqori
Harald Hermansson
Mille Kotur
Shreekara Ramesh
Joakim Tjärnlund Leppämäki

Supervisors:

Dragan Sekulic
Bengt J H Jacobson
Alexey Vdovin

January 8, 2024

Abstract

This paper is based on a project in the 2023 "Automotive Engineering Project" course at Chalmers University of Technology. As a part of a large-scale project to reduce travel times, a floating bridge is planned to be built over Bjørnafjorden on the west coast of Norway. The planned floating bridge is prone to be sensitive to environmental factors (e.g. wind and waves). Previous papers have studied the lateral stability of a bus riding over the bridge, and the Norwegian Public Roads Administration now sought an analysis of how riding over the bridge would affect bus passengers in terms of comfort and motion sickness. An existing 8 DOF bus model was extended to 13 DOF by adding a bus driver, and three passengers and also accounting for pitch motion. The model was simulated in Simulink. Accelerations from 8 axes for each bus occupant were retrieved and then weighted according to weighting filters from the ISO 2631-1. By using the mentioned ISO standard, bus users' comfort could be assessed by comparison of bus occupants' acceleration limits. Motion sickness was assessed numerically by the Motion Sickness Dose Value equation given in ISO 2631-1, however, it is a highly subjective illness.

With the 1- and 2-year storm conditions and the bus model, ride comfort and motion sickness levels were assessed. According to the received results from the simulations, it could be seen that the key contributing factors to the ride comfort were vertical and lateral accelerations. It could also be concluded that the wind forces acting on the vehicle affected the ride comfort to a great extent. The seat position and the travelling speed were also big contributors to the ride comfort. Increasing speed and a seat position away from the bus' centre of gravity had a negative impact on comfort. From a motion sickness perspective, the motions in the lower frequency range and accumulative travelling time were the main contributors. Travelling at a slower speed would negatively affect the Motion Sickness Dose Value, due to increased travelling time with motions at the low-frequency responses from the bus and bridge (e.g. wave load, current, wind excitations).

Acknowledgments

We want to thank our supervisors Bengt Jacobson, Dragan Sekulic and Alexey Vdovin for their support throughout this project. With their high knowledge in the area, they have contributed with guidance and valuable information for the progress of this project.

A big thanks are also directed towards the Chalmers simulator group Caster Chalmers for letting us work on their Cruden simulator. We want to especially thank Konrad Billing for his contribution with his knowledge and high work ethic to implement the simulator as an evaluation tool for motion sickness.

To Dragan Sekulic, Bengt Jacobson, Alexey Vdovin, Konrad Billing (Caster Chalmers), Stian Moe Johanessen (NPRA), Mats Nilsson (Volvo Group) and Edwin de Vries (Cruden B.V.) - thank you for the interesting discussions which contributed to this project and our knowledge in motion comfort and the effects on bridge construction from wind and waves.

Abbreviations

COG Center of Gravity

DOF Degrees of Freedom

EOMs Differential Equations of Motions

FBDs Free Body Diagrams

ISO International Organization for Standardization

MSDV_z Motion Sickness Dose Value (for z-axis)

NPRA Norwegian Public Roads Administration

PSD Power Spectral Density

RC Roll centre

RMS Root Mean Square

Contents

1	Introduction	1
1.1	Background	1
1.2	Purpose	2
1.3	Objectives	3
1.4	Boundaries	3
1.5	Ethics assessment	4
2	Theory	5
2.1	Vibrations on the human body	5
2.1.1	Motion sickness	7
2.1.2	Weighting filters	7
2.2	Model of the intercity bus model with users'	8
2.3	Differential equations of motion for the bus model	10
2.3.1	Assumptions	10
2.3.2	Derivation of Differential Equations of Motions (EOMs) from Free Body Diagrams (FBDs)	11
2.4	Motion platform for motion sickness assessment	25
3	Method	26
3.1	Pre-Study	26
3.2	Modelling	26
3.3	Simulations	27
3.4	Analysis	28
3.4.1	Evaluation of comfort	28
3.4.2	Evaluation of motion sickness	29
3.5	Caster implementation	29
3.5.1	Assumptions and constraints	29
4	Results	30
4.1	Simulation results for comfort	30
4.2	Simulation results for motion sickness	40
4.3	Caster implementation	42
5	Discussion	43
5.1	Discussion of ride comfort results	43
5.2	Discussion of motion sickness results	43
5.3	Future work	44
5.3.1	Testing more storm conditions	44
5.3.2	Caster implementation and blind test	44
5.3.3	Varying bus parameters	44

1 Introduction

This project is part of a large-scale project that aims to reduce travel time with new road infrastructure and a new routing between two of Norway's important industrial cities. To see whether the project is feasible there are several investigations needed. The reason for this particular project and its objectives will be described in this chapter.

1.1 Background

The Norwegian Public Roads Administration (NPRA) is currently building tunnels and bridges along the west coast of Norway to shorten the travel time between Kristiansand and Trondheim. These bridges are located on the open sea and are quite long (see Fig.1). They are exposed to various environmental factors such as storms, water displacement, and wind. The bridges are subject to movements such as sway, heave, and roll, which can have an impact on the vehicles driving on them. The bridge movements, combined with wind excitation, can cause the vehicles to experience different types of vibrations during the journey. This can make the bus occupants uncomfortable and affect drivers' driving ability. The main objective of this project is to investigate the comfort and motion sickness levels of bus occupants based on the International Organization for Standardization (ISO) 2631-1 standard on the floating bridge over Bjørnafjorden.



Figure 1: Bjørnafjorden floating bridge by COWI [1].

The stakeholder NPRA has collaborated with the Division of Vehicle Engineering and Autonomous Systems at Chalmers in previous projects concerning the floating bridge.

In the earlier projects, the assessment of driver comfort and road grip by dynamic load co-

efficient[2] have been investigated. Further, the effect of wind load and bridge motion on lateral stability [3] has also been considered.

In this project, the ride comfort of the bus driver and passengers is assessed by taking into consideration the relative seating position of the users from the Center of Gravity (COG). The mathematical model is extended to include three passengers and the driver. Further also taking the pitching motion of the bus sprung mass into consideration, a full 13 Degrees of Freedom (DOF) bus model is implemented.

1.2 Purpose

The purpose of the project is to understand the influence of environmental loads such as wind excitation and bridge motion on bus users' ride comfort and motion sickness. The comfort assessment will include different parts of the human body (e.g. feet, back and buttocks) and different directions (e.g. translation and rotational vibrations).

1.3 Objectives

The main objective of this project is to evaluate the accelerations experienced in translation and rotational directions, which can influence the comfort levels of the bus users and cause motion sickness, and how they differ depending on the seating position in the bus i.e. the relative position from COG. Additionally, this will be implemented in Caster's Cruden simulator at Chalmers University of Technology to get a perception and subjective feedback of the accelerations and how they affect the driver and the passengers. The results from the simulation will be compared to the ISO 2631-1 comfort limits.

The objectives of the project are:

- To reveal how floating bridge motion and the wind influence ride comfort and motion sickness of bus users for 1-year storm condition.
- How do drivers' and passengers' responses depend on vehicle speed and storm conditions?
- Is the ISO 2631-1 comfort limit reached on floating bridge for considered storm conditions?
- Are the comfort/motion sickness assessments from simulation comparable with subjective assessments from simulator tests?

1.4 Boundaries

Due to limitations in the amount of time that can be invested in this project and a deadline that has to be respected, there will be constraints in the project. The project will be limited according to:

- Vehicle model parameters (e.g. mass/geometric/oscillatory parameters) will be taken from the available literature.
- Simple one-mass human body models will be considered for comfort/motion sickness assessments.
- Vertical acceleration of human body masses would be considered in comfort/motion sickness assessments.
- Lateral acceleration of the vehicle's COG, pitch and roll acceleration of vehicle body would be considered in comfort/motion sickness assessments.
- Comfort/motion sickness validation process will consider results from driving simulator tests since the floating bridge is in its design phase and measurements are not possible.
- The influence of bridge obstacles (pylons and similar) on the aerodynamic forces on the studied vehicle will not primarily be included.
- The influence from vertical dynamics on-road grip is not included

1.5 Ethics assessment

The outcome of this project can have an extensive impact on the ride comfort and the safety of the driver and passengers of a bus on the floating bridge. The foundation of a reliable assessment lies in the accuracy of the physical bus model, the representations of storm conditions, and the importance of trustfulness in the bridge model. Inaccurate equations in the bus model and underestimation of the storm conditions can contribute to poor health and safety factors for the bus occupants once the bridge actually is built. Therefore, it is of great value to present truthful results to avoid health and safety issues with a floating bridge.

In order to compare the standards of ISO 2631-1, correct inputs will be used from storm conditions, and a proper bus model to simulate the bridge movement affecting the bus, and also the passengers. It is important that the project delivers reliable measurements instead of trying to prove that the ride comfort is approved according to ISO 2631-1.

The Cruden, a six-degree-of-freedom motion simulator, is a tool to assess the actual movement of the bus ride that can affect the test object badly. It is important to ensure the test objects health and safety even though they will be exposed to a movement which can cause motion sickness.

2 Theory

In the following chapter, the theory behind the project is presented. To be able to deliver a trustworthy result it is needed to provide the underlying theory and the measures that will be used for the outputs.

2.1 Vibrations on the human body

It is a widely known fact that vibrations can have adverse effects on the human body, but determining when they become uncomfortable can be difficult. To address this issue, ISO 2631-1 provides a standardized method for measuring and evaluating vibrations under various circumstances and sets specific requirements [4]. This standard will be used to evaluate the impacts of different excitations (e.g. road roughness, waves, wind, floating bridge motion) on bus users' ride comfort. The ISO 2631-1 also concerns human health, vibration perception and the incidence of motion sickness. Comfort and motion sickness will be analyzed in this project.

ISO 2631-1 specifically deals with whole-body vibration that is periodic, random, and transient. These vibrations are measured at the point of contact between the human body and the bus. For standing passengers, the vibrations are measured between their feet and the floor. For seated passengers and the driver, it is measured on the seat (between the user's buttocks and its seat), seat-backs (between the user's back and backrest) and on the floor (between the user's feet and bus floor). See figure 2 for a visualisation of the seated bus occupants.

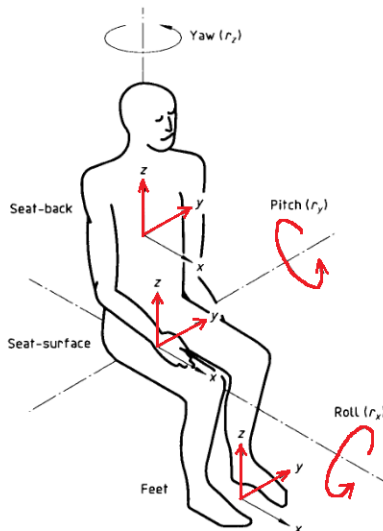


Figure 2: Seated human body with receiving points and axes [4].

Motion sickness will be evaluated at frequencies between 0.1 to 0.5 Hz, and comfort will be evaluated at frequencies between 0.5 to 80 Hz. The evaluation of comfort depends on the magnitude of the accelerations and their frequency. The various magnitudes and the causation of the driver and passengers' reactions are divided as follows, according to ISO 2631-1 [4]:

- smaller than 0.315 m/s^2 not uncomfortable
- $0.315 - 0.63 \text{ m/s}^2$ a little uncomfortable
- $0.5 - 1 \text{ m/s}^2$ fairly uncomfortable
- $0.8 - 1.6 \text{ m/s}^2$ uncomfortable
- $1.25 - 2.5 \text{ m/s}^2$ very uncomfortable
- greater than 2 m/s^2 extremely uncomfortable

These accelerations are the results of the total Root Mean Square (RMS) value for the accelerations in the different directions according to figure 2. The derived equation finally becomes:

$$\begin{aligned}
 RMS_{tot} = & ((k_{z,floor} * \ddot{z}_{w,RMS,floor})^2 + (k_{y,floor} * \ddot{y}_{w,RMS,floor})^2 + (k_{z,seat} * \ddot{z}_{w,RMS,seat})^2 + \\
 & (k_{y,seat} * \ddot{y}_{w,RMS,seat})^2 + (k_{roll,seat} * \ddot{\phi}_{w,RMS,seat})^2 + (k_{pitch,seat} * \ddot{\theta}_{w,RMS,seat})^2 + \\
 & (k_{z,seat-back} * \ddot{z}_{w,RMS,seat-back})^2 + (k_{y,seat-back} * \ddot{y}_{w,RMS,seat-back})^2)^{\frac{1}{2}} \quad (1)
 \end{aligned}$$

Where $k_{z,floor}$, $k_{y,floor}$, $k_{z,seat}$, $k_{y,seat}$, $k_{roll,seat}$, $k_{pitch,seat}$, $k_{z,seat-back}$, and $k_{y,seat-back}$ are the multiplying factors for the directional specific accelerations retrieved from the ISO 2631-1 [4] (see notation list in chapter 6). The \ddot{z}_i , \ddot{y}_i , $\ddot{\phi}_i$ and $\ddot{\theta}_i$, where index "i" represents the position-specific weighted accelerations mentioned earlier, are the RMS values.

For instance, the RMS value of the weighted vertical acceleration from users' seats is calculated by equation 2.

$$\ddot{z}_{w,RMS,seat} = \left[\frac{1}{T} \int_0^T [\ddot{z}_{w,seat}(t)]^2 dt \right]^{1/2} \quad (2)$$

where T is simulation time and $\ddot{z}_{w,seat}(t)$ is frequency weighted vertical acceleration. RMS values of the weighted acceleration for other receiving points and axes are calculated in the same way.

2.1.1 Motion sickness

The ISO 2631-1 standard [4] will be used for the assessment of the Motion Sickness Dose Value (for z-axis) (MSDV_z) for different weather conditions. According to the ISO standard, the occurrence of motion sickness is affected by the frequencies and amplitudes of the accelerations and the duration of the motion exposure. The values will be assessed according to the comparison of the different positions in the bus and dependent on the bus velocities. The MSDV_z is given by:

$$MSDV_z = \left[\int_0^T [a_w(t)]^2 dt \right]^{1/2} \quad (3)$$

Where the $a_w(t)$ is given by the frequency-weighted vertical accelerations and T is the total period where the bus user is exposed to the motions.

2.1.2 Weighting filters

The weighting filters are used for acceleration weighting to account for the human sensitivity to vibration in different directions and different frequencies. In this project, we use four weighting filters from ISO 2631-1 W_k , W_d , W_e and W_f .

- W_k is the filter curve applied to the vertical and lateral accelerations on the sprung mass at each seat's position and the vertical acceleration of the bus users. The weighted accelerations resemble the vertical and lateral accelerations a human would experience at their feet, as well as the vertical acceleration of the seat. (Figure 3)
- W_d is the filter curve applied to the vertical and lateral accelerations of the bus users. The weighted accelerations resemble the vertical and lateral accelerations a human would experience in the backrest as well as the lateral acceleration of the seat. (Figure 3).
- W_e is the filter curve applied to the angular accelerations at the seated position of the user. The weighted accelerations resemble the roll and pitch accelerations a human would experience in the seat. (Figure 4).
- W_f is the filter curve applied to the vertical accelerations of the bus users for motion sickness assessment. The weighted accelerations are the vertical accelerations that affect the motion sickness of humans. (Figure 3)

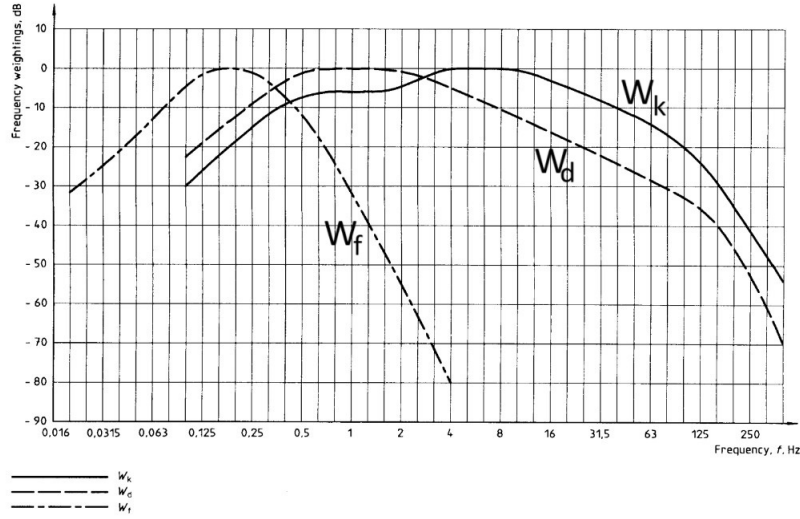


Figure 3: Frequency weighting curve for principal weightings [4].

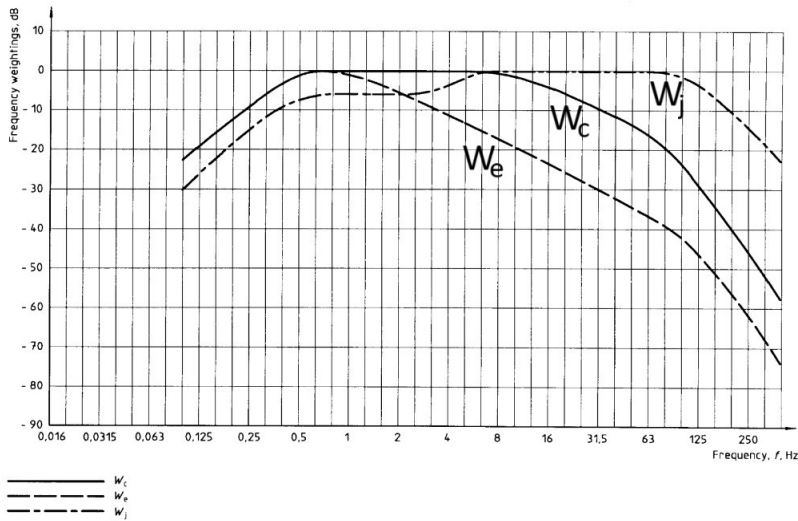


Figure 4: Frequency weighting curve for additional weightings [4].

2.2 Model of the intercity bus model with users'

To derive the differential equations for out-of-road-plane motions, FBDs of the bus were defined. Figure 5 shows the location of the driver and the passengers, as well as the spring and damper parameters in the extended bus model. From this, the forces and lengths will in a later stage be visualized for the EOMs. The values of the parameters can be seen in chapter 6.

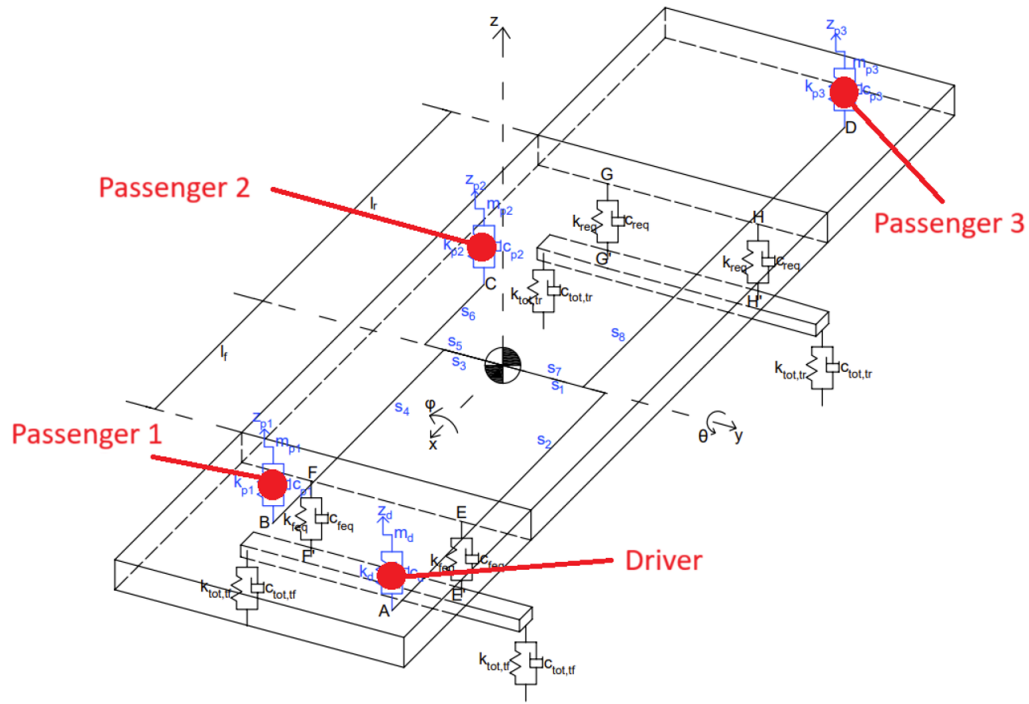


Figure 5: Schematic diagram of the bus.

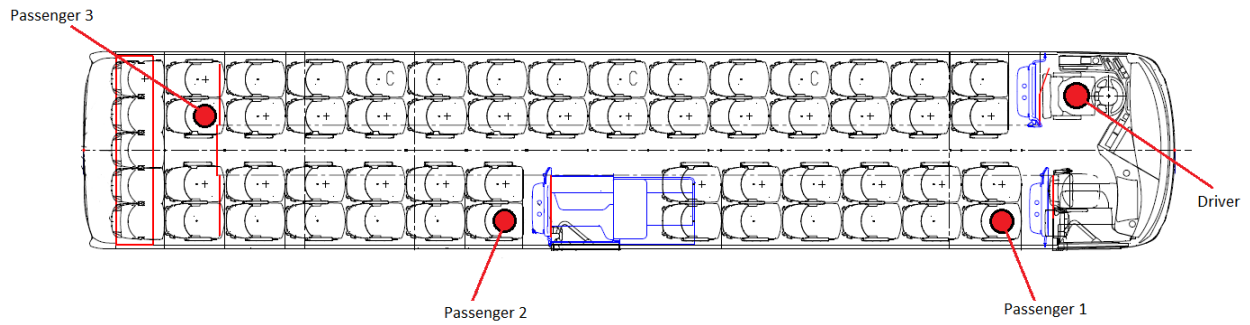


Figure 6: Driver and passengers' seat locations.

2.3 Differential equations of motion for the bus model

To evaluate the bus user's comfort, the most important values to retrieve and analyze from the simulations are the vertical, lateral and angular accelerations of the bus users.

This chapter therefore describes the differential equations that have been derived from FBDs, which were necessary to mathematically describe the mechanical system of 13 DOF.

2.3.1 Assumptions

The assumptions below are retrieved from [3]:

- The bus is driving at a constant longitudinal speed.
- The bus is symmetrical relative to the X-axis around the COG.
- Linear characteristics are used for all spring and damper elements.
- The bus body and axles are rigid bodies.
- The axles are attached to the bus body, but can still roll and bounce with respect to it.
- Since the mass of the bus body is considerably higher than the masses of the bus axles, the COG of the sprung mass is assumed to coincide with the COG of the total vehicle.
- The Roll centre (RC)s of the front and rear axle coincides with their own COG.
- The suspension forces are determined concerning the static position, meaning that the gravity terms can be omitted in the force equilibrium equations.
- All possible motions of concentrated masses around the position of stationary equilibrium are small.

2.3.2 Derivation of EOMs from FBDs

According to figure 7, the vertical force equilibrium governing the bus seats corresponds to equation 4.

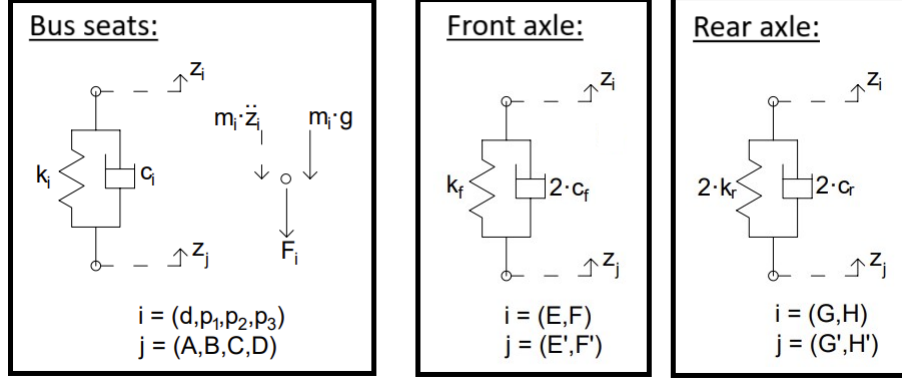


Figure 7: Free body diagram of bus seats' and axles' suspension system.

$$-F_i - m_i \ddot{z}_i = 0 \quad (4)$$

where the subscript $i = (d, p_1, p_2, p_3)$ is for the driver, passenger 1, passenger 2 and passenger 3, respectively. m_i is the mass of the specific bus user and \ddot{z}_i is the vertical acceleration of the specific bus user. Weight terms ($m_i g$) do not appear in equation 4 since the coordinate systems for vertical directions were placed in point masses static equilibrium positions.

Equations 5 to 8 present the magnitudes of the suspension forces (F_i) from the seats of the driver and passengers.

$$F_d = c_d(\dot{z}_d - \dot{z}_A) + k_d(z_d - z_A) \quad (5)$$

$$F_{p1} = c_{p1}(\dot{z}_{p1} - \dot{z}_B) + k_{p1}(z_{p1} - z_B) \quad (6)$$

$$F_{p2} = c_{p2}(\dot{z}_{p2} - \dot{z}_C) + k_{p2}(z_{p2} - z_C) \quad (7)$$

$$F_{p3} = c_{p3}(\dot{z}_{p3} - \dot{z}_D) + k_{p3}(z_{p3} - z_D) \quad (8)$$

c and k are the seats' damping and spring stiffness coefficients, respectively. z_d, z_{p1}, z_{p2} and z_{p3} are the vertical motions of the bus users. z_A, z_B, z_C and z_D describe the vertical motion of the point where their seats are connected to the bus floor, see equations 9 to 12. They depend on the sprung mass vertical motion, z_s , as well as the sprung mass roll and pitch motions, ϕ_s and θ_s .

$$z_A = z_s + s_1\dot{\phi}_s - s_2\dot{\theta}_s \quad (9)$$

$$z_B = z_s - s_3\dot{\phi}_s - s_4\dot{\theta}_s \quad (10)$$

$$z_C = z_s - s_5\dot{\phi}_s + s_6\dot{\theta}_s \quad (11)$$

$$z_D = z_s + s_7\dot{\phi}_s + s_8\dot{\theta}_s \quad (12)$$

where s_1, s_3, s_5 and s_7 (odd numbers) are the lateral distances from the bus users' seats to COG, while s_2, s_4, s_6 and s_8 (even numbers) are the longitudinal distances from the bus users' seats to COG. See figure 8 for a visual presentation of the seats' placements.

Given equations 4, 5 and 9, the EOM for the bus driver is given by equations 13, 14 and 15:

$$m_d\ddot{z}_d = -F_d \quad (13)$$

$$m_d\ddot{z}_d = -c_d(\dot{z}_d - \dot{z}_A) - k_d(z_d - z_A) \quad (14)$$

$$m_d\ddot{z}_d = -c_d(\dot{z}_d - \dot{z}_s - s_1\dot{\phi}_s + s_2\dot{\theta}_s) - k_d(z_d - z_s - s_1\phi_s + s_2\theta_s) \quad (15)$$

Using the same strategy for all the other bus users, the final forms of the EOMs for the bus users could be retrieved, see equations 16-19.

Driver:

$$m_d\ddot{z}_d + c_d\dot{z}_d + k_d z_d - c_d\dot{z}_s - k_d z_s - s_1 c_d \dot{\phi}_s - s_1 k_d \phi_s + s_2 c_d \dot{\theta}_s + s_2 k_d \theta_s = 0 \quad (16)$$

Passenger 1:

$$m_{p1}\ddot{z}_{p1} + c_{p1}\dot{z}_{p1} + k_{p1}z_{p1} - c_{p1}\dot{z}_s - k_{p1}z_s + s_3 c_{p1} \dot{\phi}_s + s_3 k_{p1} \phi_s + s_4 c_{p1} \dot{\theta}_s + s_4 k_{p1} \theta_s = 0 \quad (17)$$

Passenger 2:

$$m_{p2}\ddot{z}_{p2} + c_{p2}\dot{z}_{p2} + k_{p2}z_{p2} - c_{p2}\dot{z}_s - k_{p2}z_s + s_5 c_{p2} \dot{\phi}_s + s_5 k_{p2} \phi_s - s_6 c_{p2} \dot{\theta}_s - s_6 k_{p2} \theta_s = 0 \quad (18)$$

Passenger 3:

$$m_{p3}\ddot{z}_{p3} + c_{p3}\dot{z}_{p3} + k_{p3}z_{p3} - c_{p3}\dot{z}_s - k_{p3}z_s - s_7 c_{p3} \dot{\phi}_s - s_7 k_{p3} \phi_s - s_8 c_{p3} \dot{\theta}_s - s_8 k_{p3} \theta_s = 0 \quad (19)$$

Equation 20 describes the vertical force equilibrium of the sprung mass retrieved from figure 8.

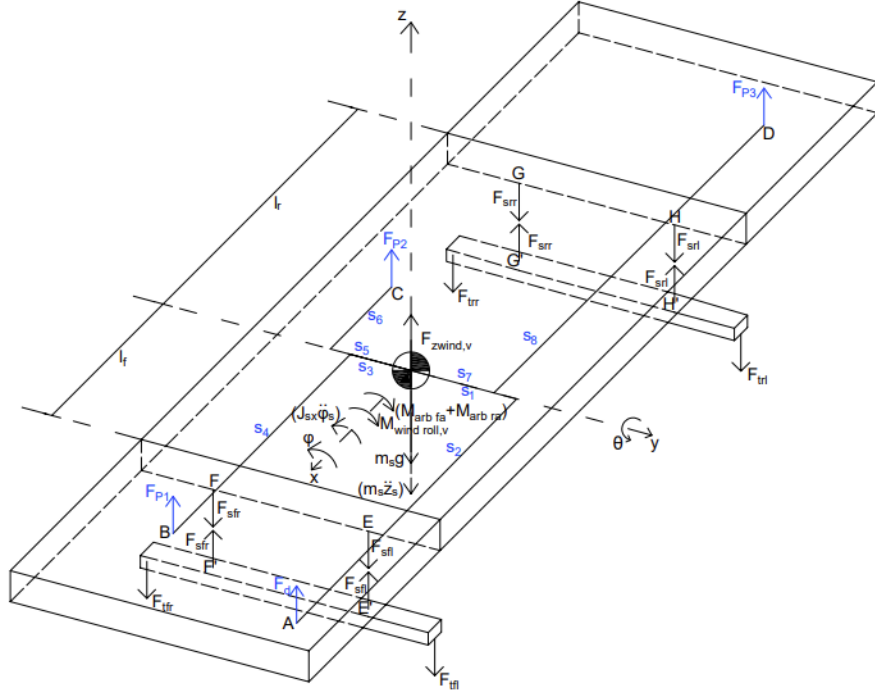


Figure 8: Free body diagram of the bus with vertical forces.

$$m_s \ddot{z}_s - F_d - F_{p1} - F_{p2} - F_{p3} + F_{sfl} + F_{sfr} + F_{srr} + F_{srl} - F_{zwind,v} = 0 \quad (20)$$

where m_s is the sprung mass and \ddot{z}_s is its vertical acceleration. F_{sfl} , F_{sfr} , F_{srr} and F_{srl} are the forces from the bus suspension system. The magnitude of these forces could be determined from figure 7, see equations 21-24. $F_{zwind,v}$ is the vertical component of the aerodynamic loads and is described by equation 66.

$$F_{sfl} = 2c_f(\dot{z}_E - \dot{z}_{E'}) + k_f(z_E - z_{E'}) \quad (21)$$

$$F_{sfr} = 2c_f(\dot{z}_F - \dot{z}_{F'}) + k_f(z_F - z_{F'}) \quad (22)$$

$$F_{srr} = 2c_r(\dot{z}_G - \dot{z}_{G'}) + 2k_r(z_G - z_{G'}) \quad (23)$$

$$F_{srl} = 2c_r(\dot{z}_H - \dot{z}_{H'}) + 2k_r(z_H - z_{H'}) \quad (24)$$

The force equations above include new subscripts for vertical motions. z_E , z_F , z_G and z_H denote the vertical motion of the point where the suspension units are connected to the sprung mass. $z_{E'}$, $z_{F'}$, $z_{G'}$, and $z_{H'}$ describe the vertical motion of the point where the suspension units are connected to the axles (unsprung masses). c_f , k_f , c_r and k_r are the frontal and rear axles' suspension damping and spring stiffness coefficients for a single element. See equations 25-32 for the motion of these points and also figure 8 for their locations in the FBD.

$$z_E = z_s + e_{uf}\phi_s - l_f\theta_s \quad (25)$$

$$z_F = z_s - e_{uf}\phi_s - l_f\theta_s \quad (26)$$

$$z_G = z_s - e_{ur}\phi_s + l_r\theta_s \quad (27)$$

$$z_H = z_s + e_{ur}\phi_s + l_r\theta_s \quad (28)$$

$$z_{E'} = z_{uf} + e_{uf}\phi_{uf} \quad (29)$$

$$z_{F'} = z_{uf} - e_{uf}\phi_{uf} \quad (30)$$

$$z_{G'} = z_{ur} - e_{ur}\phi_{ur} \quad (31)$$

$$z_{H'} = z_{ur} + e_{ur}\phi_{ur} \quad (32)$$

The subscripts uf and ur are introduced for the unsprung mass on the front axle and the unsprung mass on the rear axle. l_f and l_r are the longitudinal distances between front/rear axle to COG. e_{uf} and e_{ur} are the lateral distances between axle COG and the suspension elements for the front and the rear axles, respectively.

By combining equations 5-12 and 20-32, the final form of the EOM for the bus sprung mass vertical motion could be retrieved, see equation 33.

$$\begin{aligned}
m_s \ddot{z}_s + (c_d + c_{p1} + c_{p2} + c_{p3} + 4c_f + 4c_r) \dot{z}_s + (k_d + k_{p1} + k_{p2} + k_{p3} + 2k_f + 4k_r) z_s \\
+ (s_1 c_d - s_3 c_{p1} - s_5 c_{p2} + s_7 c_{p3}) \dot{\phi}_s + (s_1 k_d - s_3 k_{p1} - s_5 k_{p2} + s_7 k_{p3}) \phi_s \\
- (s_2 c_d + s_4 c_{p1} - s_6 c_{p2} - s_8 c_{p3} + 4l_f c_f - 4l_r c_r) \dot{\theta}_s \\
- (s_2 k_d + s_4 k_{p1} - s_6 k_{p2} - s_8 k_{p3} + 2l_f k_f - 4l_r k_r) \theta_s \\
- c_d \dot{z}_d - k_d z_d - c_{p1} \dot{z}_{p1} - k_{p1} z_{p1} - c_{p2} \dot{z}_{p2} - k_{p2} z_{p2} - c_{p3} \dot{z}_{p3} - k_{p3} z_{p3} \\
- 4c_f \dot{z}_{uf} - 2k_f z_{uf} - 4c_r \dot{z}_{ur} - 4k_r z_{ur} - F_{zwind,v} = 0
\end{aligned} \tag{33}$$

Equation 34 describes the moment equilibrium around the x-axis (roll motion) based on the FBD seen in figure 9.

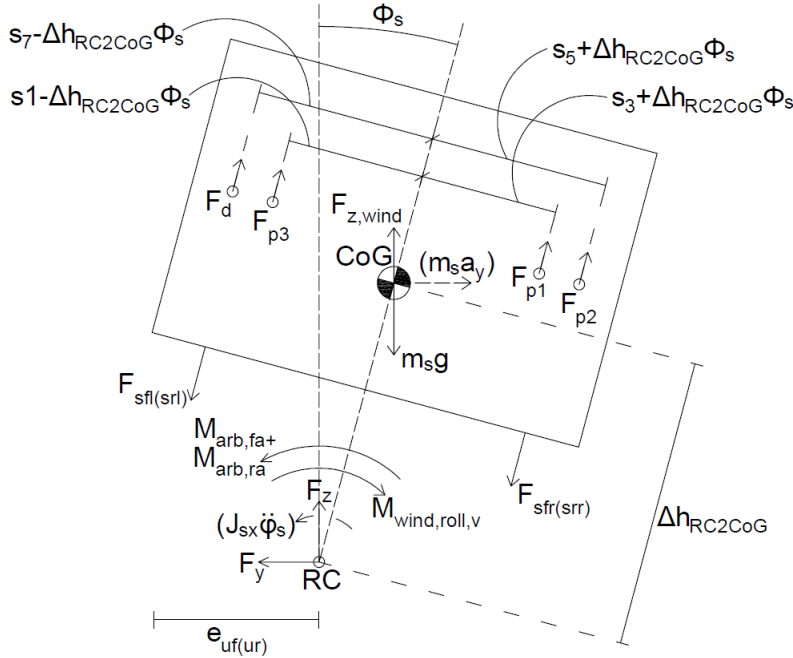


Figure 9: Free body diagram of the sprung mass roll on the bus.

$$\begin{aligned}
J_{sx}\ddot{\phi}_s - (m_s g - F_{z,wind})\Delta h_{RC2CoG}\phi_s - m_s a_y \Delta h_{RC2CoG} \\
- (F_{sfr} - F_{sfl})e_{uf} - (F_{srr} - F_{srl})e_{ur} \\
+ M_{arb,fa} + M_{arb,ra} - M_{windroll,v} \\
- F_d(s_1 - \Delta h_{RC2CoG}\phi_s) \\
- F_{p3}(s_7 - \Delta h_{RC2CoG}\phi_s) + F_{p1}(s_3 + \Delta h_{RC2CoG}\phi_s) \\
+ F_{p2}(s_5 + \Delta h_{RC2CoG}\phi_s) = 0
\end{aligned} \tag{34}$$

J_{sx} is the sprung mass moment of inertia around the x-axis. Δh_{RC2CoG} is the vertical distance from COG to the vehicle roll-axis. a_y is the lateral acceleration of the sprung mass. $M_{windroll,v}$ is the roll moment component from the aerodynamic loads (see equation 67). $M_{arb,fa}$ and $M_{arb,ra}$ are the moments created due to the anti-roll bars on the front and rear axles, see equations 35 and 36.

$$M_{arb,fa} = k_{arb,f}(\phi_s - \phi_{uf}) \tag{35}$$

$$M_{arb,ra} = k_{arb,r}(\phi_s - \phi_{ur}) \tag{36}$$

where $k_{arb,f}$ and $k_{arb,r}$ are stiffness coefficients for the front and rear anti-roll bars, respectively.

Equation 37 describes the moment equilibrium around the y-axis (pitch motion) based on the FBD seen in figure 10.

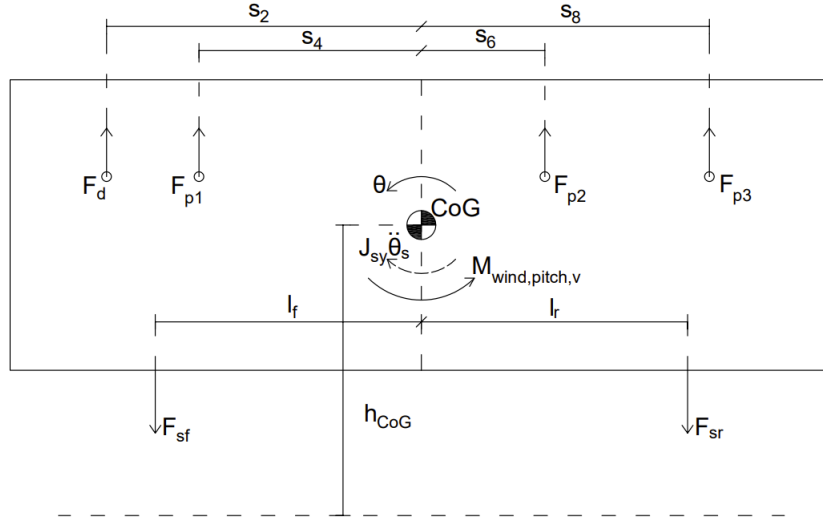


Figure 10: Free body diagram of the sprung mass pitch on the bus.

$$J_{sy}\ddot{\theta}_s + F_d s_2 + F_{p1} s_4 - F_{p2} s_6 - F_{p3} s_8 - (F_{sfl} + F_{sfr})l_f + (F_{srr} + F_{srl})l_r - M_{windpitch,v} = 0 \quad (37)$$

where J_{sy} is the sprung mass moment of inertia around the y-axis and $M_{windpitch,v}$ is the pitch moment component from the aerodynamic loads (see equation 68). As the bus is driving with a constant longitudinal speed, there is no force component from longitudinal acceleration.

By combining equation 37 with equations 5 - 12 and 21 - 32, the final form of the EOM for the sprung mass pitch moment can be retrieved, see equation 38.

$$\begin{aligned} & J_{sy}\ddot{\theta}_s + (s_2^2 c_d + s_4^2 c_{p1} + s_6^2 c_{p2} + s_8^2 c_{p3} + 4c_f l_f^2 + 4c_r l_r^2)\dot{\theta}_s \\ & \quad + (s_2^2 k_d + s_4^2 k_{p1} + s_6^2 k_{p2} + s_8^2 k_{p3} + 2k_f l_f^2 + 4k_r l_r^2)\theta_s \\ & \quad + s_2 c_d \dot{z}_d + s_2 k_d z_d + s_4 c_{p1} \dot{z}_{p1} + s_4 k_{p1} z_{p1} - s_6 c_{p2} \dot{z}_{p2} - s_6 k_{p2} z_{p2} - s_8 c_{p3} \dot{z}_{p3} - s_8 k_{p3} z_{p3} \\ & \quad \quad - (s_2 c_d + s_4 c_{p1} - s_6 c_{p2} - s_8 c_{p3} + 4c_f l_f - 4c_r l_r)\dot{z}_s \\ & \quad \quad - (s_2 k_d + s_4 k_{p1} - s_6 k_{p2} - s_8 k_{p3} + 2k_f l_f - 4k_r l_r)z_s \\ & \quad - (s_1 s_2 c_d - s_3 s_4 c_{p1} + s_5 s_6 c_{p2} - s_7 s_8 c_{p3})\dot{\phi}_s - (s_1 s_2 k_d - s_3 s_4 k_{p1} + s_5 s_6 k_{p2} - s_7 s_8 k_{p3})\phi_s \\ & \quad \quad + 4c_f l_f \dot{z}_{uf} + 2k_f l_f z_{uf} - 4c_r l_r \dot{z}_{ur} - 4k_r l_r z_{ur} \\ & \quad \quad \quad - M_{windpitch,v} = 0 \end{aligned} \quad (38)$$

The whole vehicle's lateral force equilibrium and moment equilibrium around the Z-axis (Yaw motion) are described by equations 39 and 40.

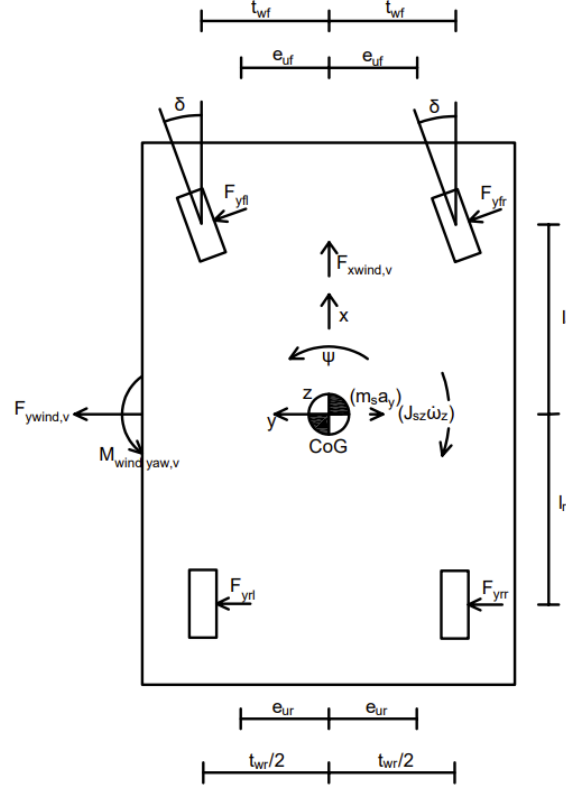


Figure 11: Free body diagram of the lateral motion and yaw motion on the bus.

$$m_s(\dot{v}_y + v_x\omega_z) - F_{yfl}\cos\delta - F_{yfr}\cos\delta - F_{yrl} - F_{yrr} - F_{ywind,v} = 0 \quad (39)$$

$$J_{sz}\dot{\omega}_z - (F_{yfl} - F_{yfr})\sin\delta\frac{tw_f}{2} - (F_{yfl} + F_{yfr})\cos\delta l_f + (F_{yrl} + F_{yrr})l_r - M_{windyaw,v} = 0 \quad (40)$$

v_x and v_y are the vehicle's velocities in the longitudinal and lateral directions, and ω_z is its angular velocity around the z-axis (yaw rate). δ is the steering angle of the road wheels. tw_f is the track width of the front axle. F_{yfl} , F_{yfr} , F_{yrl} , and F_{yrr} are the lateral forces on the tyres and were already given in the existing Simulink model (see [3] for how they are derived). $F_{ywind,v}$ and $M_{windyaw,v}$ are the aerodynamic loads described by equations 65 and 69.

Equations 41 and 42 describe the vertical force equilibrium and the moment equilibrium around the x-axis (roll motion) for the front axle, based on the FBD seen in figure 12.

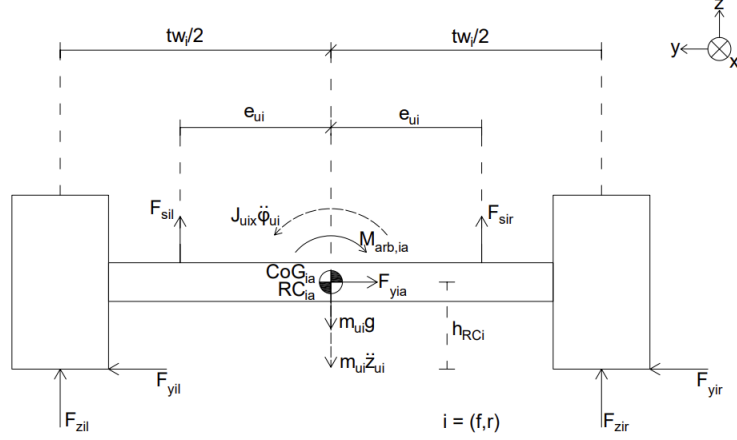


Figure 12: Free body diagram of the axles of the bus.

$$m_{uf}\ddot{z}_{uf} - F_{sfl} - F_{sfr} - F_{zfl} - F_{zfr} + m_{uf}g = 0 \quad (41)$$

$$J_{ufx}\ddot{\phi}_{uf} + (F_{sfr} - F_{sfl})e_{uf} + (F_{zfr} - F_{zfl})\frac{tw_f}{2} - (F_{yfr} + F_{yfl})\cos\delta h_{RCf} - M_{arb,fa} = 0 \quad (42)$$

where m_{uf} and \ddot{z}_{uf} are the mass and the vertical acceleration of the front axle. J_{ufx} is the moment of inertia, $\ddot{\phi}_{uf}$ the roll acceleration and h_{RCf} the roll center height. All of them are for the front axle. F_{yfr} and F_{yfl} are the lateral tyre forces on the front axle, that are calculated by using the brush tyre model. The brush tyre model can be found in [5]. F_{zfl} and F_{zfr} are the total vertical forces on each of the tyres on the front axle. Equations 43 and 44 describe them according to [3].

$$F_{zfl} = F_{zfl,st} - \frac{\Delta Z_{Mwind,pitch,v}}{2} - F_{zfl,dyn} \quad (43)$$

$$F_{zfr} = F_{zfr,st} - \frac{\Delta Z_{Mwind,pitch,v}}{2} - F_{zfr,dyn} \quad (44)$$

where $F_{zfl,st}$ and $F_{zfr,st}$ are the static tyre vertical forces on the front axle and $F_{zfl,dyn}$ and $F_{zfr,dyn}$ are the dynamic vertical forces on the front axle (see equations 45 and 46 for their

magnitudes). The vertical load denoted as $\Delta Z_{Mwind,pitch,v}$, represents the transfer of weight from the front to the rear axle caused by the pitching moment induced by wind.

$$F_{zfl,dyn} = k_{tf}(z_{uf} + \frac{tw_f}{2}\phi_{uf} - \xi_{fl}) \quad (45)$$

$$F_{zfr,dyn} = k_{tf}(z_{uf} - \frac{tw_f}{2}\phi_{uf} - \xi_{fr}) \quad (46)$$

where ξ is the road roughness value for the relevant contact patch (see their subscripts), while k_{tf} is a single tyre's stiffness on the front axle.

The magnitude of the static vertical forces and the load transfer terms are equal to the weight term in equation 41, which means that the vertical force equilibrium can be rewritten as equation 47.

$$m_{uf}\ddot{z}_{uf} - F_{sfl} - F_{sfr} + F_{zfl,dyn} + F_{zfr,dyn} = 0 \quad (47)$$

Combining equations 21, 22, 45, 46 and 47 give the final form of the front axles heave EOM seen in equation 48.

$$\begin{aligned} m_{uf}\ddot{z}_{uf} + 4c_f\dot{z}_{uf} + 2(k_f + k_{tf})z_{uf} - 4c_f\dot{z}_s - 2k_fz_s \\ + 4c_f l_f \dot{\theta}_s + 2k_f l_f \theta_s - k_{tf}\xi_{fl} - k_{tf}\xi_{fr} = 0 \end{aligned} \quad (48)$$

The final form of the front axle roll moment EOM can be seen in equation 49, retrieved from [3].

$$\begin{aligned} J_{ufx}\ddot{\phi}_{uf} - c_{\phi,f}(\dot{\phi}_s - \dot{\phi}_{uf}) - k_{\phi,f}(\phi_s - \phi_{uf}) - (F_{yfr} + F_{yfl})\cos\delta h_{RCf} \\ - k_{tf}\frac{tw_f}{2}(z_{uf} - \frac{tw_f}{2}\phi_{uf} - \xi_{fr}) + k_{tf}\frac{tw_f}{2}(z_{uf} + \frac{tw_f}{2}\phi_{uf} - \xi_{fl}) \\ - k_{arb,f}(\phi_s - \phi_{uf}) = 0 \end{aligned} \quad (49)$$

where $k_{\phi,f}$ and $c_{\phi,f}$ are the roll stiffness and roll damping for the front axle, respectively. They are described by equations 50 and 51.

$$k_{\phi,f} = \frac{1}{2}k_f(2e_{uf})^2 \quad (50)$$

$$c_{\phi,f} = \frac{1}{2}2c_f(2e_{uf})^2 = c_f(2e_{uf})^2 \quad (51)$$

Similarly, the rear axle's force and moment equilibrium equations were made from the FBD in figure 12, but with relevant subscripts. See equations 52 and 53.

$$m_{ur}\ddot{z}_{ur} - F_{srr} - F_{srl} - F_{zrl} - F_{zrr} + m_{ur}g = 0 \quad (52)$$

$$J_{urx}\ddot{\phi}_{ur} + (F_{srr} - F_{srl})e_{ur} + (F_{zrr} - F_{zrl})\frac{tw_r}{2} - (F_{yrr} + F_{yrl})h_{RCr} - M_{arb,ra} = 0 \quad (53)$$

where F_{yrr} and F_{yrl} are the lateral tyre forces on the rear axle. Again, calculated by using the brush tyre model [5]. F_{zrl} and F_{zrr} are the total vertical forces on each of the tyres on the rear axle. Equations 54 and 55 describe them according to [3].

$$F_{zrl} = F_{zrl,st} + \frac{\Delta Z_{Mwind,pitch,v}}{2} - F_{zrl,dyn} \quad (54)$$

$$F_{zrr} = F_{zrr,st} + \frac{\Delta Z_{Mwind,pitch,v}}{2} - F_{zrr,dyn} \quad (55)$$

where $F_{zrl,st}$ and $F_{zrr,st}$ are the static tyre vertical forces on the rear axle and $F_{zrl,dyn}$ and $F_{zrr,dyn}$ are the dynamic vertical forces on the rear axle (see equations 56 and 57 for their magnitudes).

$$F_{zrl,dyn} = k_{tr}(z_{ur} + \frac{tw_r}{2}\phi_{ur} - \xi_{rl}) \quad (56)$$

$$F_{zrr,dyn} = k_{tr}(z_{ur} - \frac{tw_r}{2}\phi_{ur} - \xi_{rr}) \quad (57)$$

where ξ is the road roughness value for the relevant contact patch (see their subscripts), while k_{tr} is a single tyre's stiffness on the rear axle.

The magnitude of the static vertical forces and the load transfer terms are again equal to the weight term in equation 52, which means that the vertical force equilibrium can be rewritten as equation 58.

$$m_{ur}\ddot{z}_{ur} - F_{srl} - F_{srr} + F_{zrl,dyn} + F_{zrr,dyn} = 0 \quad (58)$$

Combining equations 23, 24, 56, 57 and 58 gives the final form of the rear axles heave EOM in equation 59.

$$\begin{aligned} m_{ur}\ddot{z}_{ur} + 4c_r\dot{z}_{ur} + 2(2k_r + k_{tr})z_{ur} - 4c_r\dot{z}_s - 4k_r z_s \\ + 4c_r l_r \dot{\theta}_s + 4k_r l_r \theta_s - k_{tr}\xi_{rr} - k_{tr}\xi_{rl} = 0 \end{aligned} \quad (59)$$

The final form of the rear axle roll moment EOM can also be retrieved from [3], see equation 60.

$$\begin{aligned} J_{urx}\ddot{\phi}_{ur} - c_{\phi,r}(\dot{\phi}_s - \dot{\phi}_{ur}) - k_{\phi,r}(\phi_s - \phi_{ur}) - (F_{yrr} + F_{yrl})h_{RCr} \\ - k_{tr}\frac{tw_r}{2}(z_{ur} - \frac{tw_r}{2}\phi_{ur} - \xi_{rr}) + k_{tr}\frac{tw_r}{2}(z_{ur} + \frac{tw_r}{2}\phi_{ur} - \xi_{rl}) \\ - k_{arb,r}(\phi_s - \phi_{ur}) = 0 \end{aligned} \quad (60)$$

where $k_{\phi,r}$ and $c_{\phi,r}$ are the roll stiffness and roll damping for the rear axle, respectively. They are described by equations 61 and 62.

$$k_{\phi,r} = \frac{1}{2}2k_r(2e_{ur})^2 = k_r(2e_{ur})^2 \quad (61)$$

$$c_{\phi,r} = \frac{1}{2}2c_r(2e_{ur})^2 = c_r(2e_{ur})^2 \quad (62)$$

2.3.2.1 Lateral accelerations of bus users

The lateral accelerations of the bus users were not included in the DOFs of this model due to the assumption that the seats could only move in the vertical plane relative to the bus. But for the assessment, the lateral accelerations of the users could be calculated by using other simulated accelerations of the bus. Equation 63 describes how the lateral acceleration of passenger 1's seat surface was calculated.

$$\ddot{y}_{p1} = \ddot{y}_s + \ddot{\psi}_s \sqrt{s_3^2 + s_4^2} + \ddot{\phi}_s \sqrt{h_{p1}^2 + s_3^2} \quad (63)$$

where \ddot{y}_s is the sprung mass' lateral acceleration, $\ddot{\psi}_s$ the sprung mass's yaw acceleration and $\ddot{\phi}_s$ the sprung mass's roll acceleration. h_{p1} is the seat's vertical distance from the COG of the bus.

2.3.2.2 Aerodynamic loads calculation

Since the wind can have a significant effect, the wind forces and moments acting on the bus have to be calculated. From figure 13 equation (64)-(69) can be constructed. These end up exactly the same as equations (38)-(43) in [3].

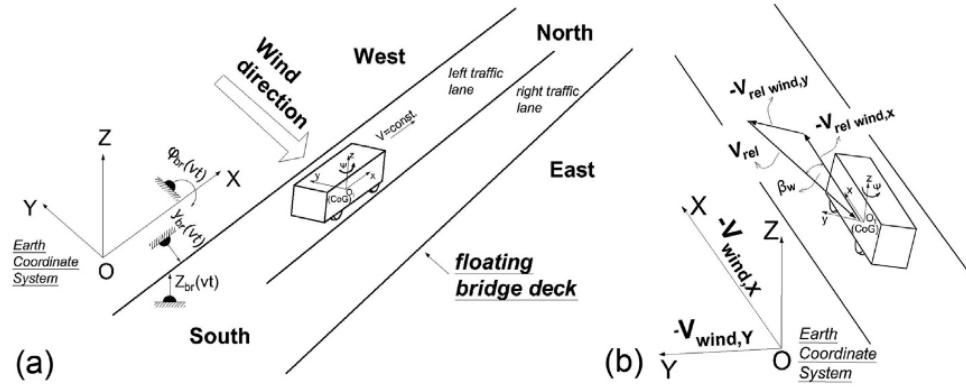


Figure 13: a) Earth (OXYZ) and vehicle (O1xyz) coordinate systems; b) wind velocity components [3].

$$F_{xwind,v} = \text{sign}(V_{relwind,x}) \frac{1}{2} \rho V_{rel}^2 AC_d(\beta_w) \quad (64)$$

$$F_{ywind,v} = \text{sign}(V_{relwind,y}) \frac{1}{2} \rho V_{rel}^2 AC_s(\beta_w) \quad (65)$$

$$F_{zwind,v} = \frac{1}{2}\rho V_{rel}^2 AC_l(\beta_w) \quad (66)$$

$$M_{windroll,v} = -\frac{1}{2}\rho V_{rel}^2 AL(C_r(\beta_w) + \frac{h_{CoG} - \Delta h_{sm}}{L}C_s(\beta_w)) \quad (67)$$

$$M_{windpitch,v} = -\frac{1}{2}\rho V_{rel}^2 AL(C_p(\beta_w) + \frac{l_f - \frac{L}{2}}{L}C_l(\beta_w) - \frac{h_{CoG}}{L}C_d(\beta_w)) \quad (68)$$

$$M_{windyaw,v} = \frac{1}{2}\rho V_{rel}^2 AL(C_Y(\beta_w) - \frac{l_f - \frac{L}{2}}{L}C_s(\beta_w)) \quad (69)$$

Where ρ is the density of air, V_{rel} is the relative velocity between the wind and the bus, A is the frontal area of the bus, L is the wheelbase length, C_d , C_s , C_l , C_R , C_P and C_Y are the aerodynamic coefficients which are functions of the wind yaw attack angle β_w . These can be extracted from figure 14 sourced from [3].

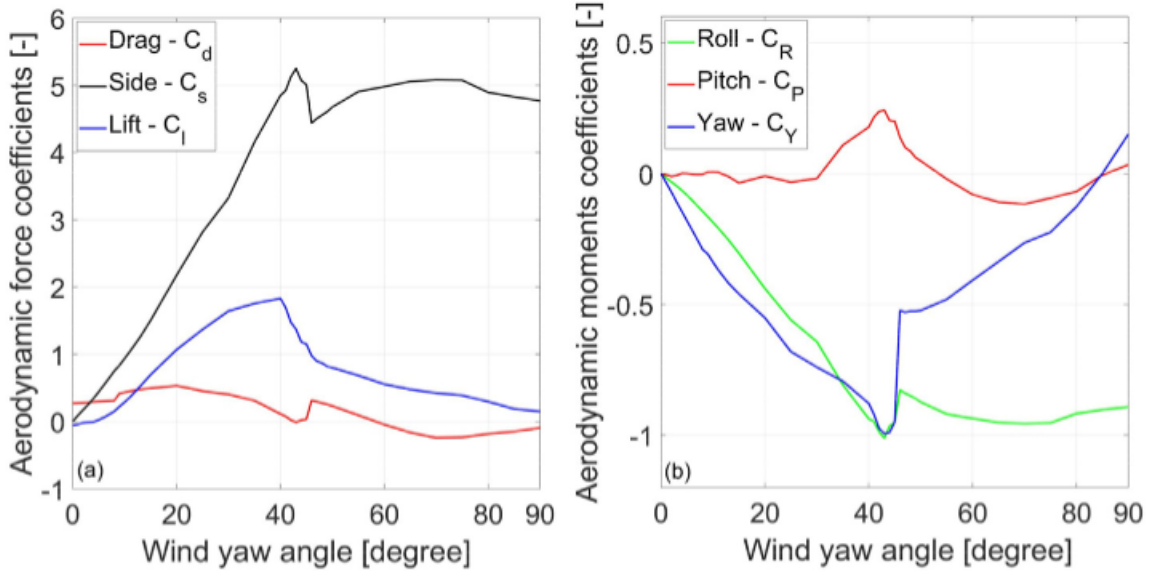


Figure 14: Aerodynamic coefficients for a) forces; b) moments as a function of the wind yaw angle [3].

2.4 Motion platform for motion sickness assessment

For the evaluation of motion sickness, a motion platform can be used. The motion platform contributes with a perception to the subjective feeling of motion sickness. It can be used as a complement to the assessment according to ISO 2631-1.

In figure 15, the motion platform can be seen. The intended motion platform that will be used is an automotive driving simulator from Cruden B.V [6]. It is a 6 DOF motion system which is used as a driver-in-the-loop evaluation for vehicle dynamic testing.



Figure 15: The Cruden 6 DOF simulator used for a driver-in-the-loop, here for vehicle dynamics evaluation of a racing vehicle.

The 6 DOF simulator that will be used for the project is situated at Chalmers University of Technology. It is under the control of the student community Caster Chalmers, which is based on the Mechanical Engineering Program [7]. The board members of the student community Caster are knowledge-bearing regarding the motion system implementation in the Cruden platform.

3 Method

In this chapter, the method for the project will be presented. It will cover all the steps from pre-study, modelling, simulation and analysis, as well as the Caster implementation for subjective testing of the comfort and motion sickness.

3.1 Pre-Study

The first stage of the project was to obtain knowledge about the problem and what had been done before. There have been several papers written about the Norwegian floating bridge project, as well as the bus user comfort. The two main papers that were studied were "Effects of wind loads and floating bridge motion on intercity bus lateral stability" (Sekulić, D. et al. 2021) [3] and "Analysis of vibration effects on the comfort of intercity bus users by oscillatory model with ten degrees of freedom" (Sekulić, D. et al. 2013) [2].

The titles are quite self-explanatory, but the first one is an analysis of how a bus will be affected by wind and water when driving over the same bridge as this project is based on. The second one describes bus user's comfort when driving in a straight line at a constant speed. These papers were especially useful to the project because their ideas could be combined to solve the problem, as passengers and drivers were added to the bus model driving on the floating bridge in Norway.

3.2 Modelling

The Simulink model used in [3] was given to the group, however, changes had to be made to retrieve the necessary results from the simulations. 5 degrees of freedom were added to the existing 8 DOF bus model. The 8 original ones were:

1. Heave motion of sprung mass
2. Heave motion of the front axle
3. Heave motion of the rear axle
4. Roll motion of the sprung mass
5. Roll motion of the front axle
6. Roll motion of the rear axle
7. Lateral motion of the entire vehicle
8. Yaw motion of the entire vehicle

To study the comfort of bus user's, one driver and three passengers were added to the model based on [2].

9. Heave motion of the driver

10. Heave motion of passenger 1
11. Heave motion of passenger 2
12. Heave motion of passenger 3

The last DOF that was added was the pitch motion of the bus body. It was not considered in the original model, but a more detailed model was needed to reflect different passenger positions.

13. Pitch motion of the bus body

Most of the necessary EOMs already existed in the Simulink model but had to be edited to add the new DOFs. FBDs were created to derive the new EOMs that were needed to balance the system of equations. As the existing Simulink model was based on [3], it already contained equations describing the bus excitations like the wind and the bridge movement.

The Simulink model (and this report) contained a lot of parameters and variables. A list of notations was therefore made to conveniently keep track of them. It was essential to do this as the papers from the pre-study used different notations for the same vehicle variable/parameter.

The relevant equations for this project can be seen in the theory chapter 2.3. The list of notations can be seen in appendix 6.

3.3 Simulations

The simulations were carried out with the help of Matlab and the extension Simulink. The EOMs were implemented in Simulink and thus the parameters could be assigned from a Matlab script and results were derived.

An existing driver model from [3] was used in the simulation to keep the bus driving in its lane. It was simulated for five different, constant longitudinal velocities:

- 36 km/h
- 54 km/h
- 72 km/h
- 90 km/h
- 108 km/h

The model was simulated with and without wind forces acting on the bus. These two conditions could be used to evaluate the influence of the wind on the bus. The model was mainly simulated for a 1-year storm condition, however, a higher intensity 2-year storm condition was also used later on. This was to perceive whether the simulation worked well

and also how much the ride comfort would decrease and the motion sickness would increase for a worse scenario.

3.4 Analysis

After simulating the model on Simulink, the effects of the following accelerations were analysed by applying the respective weighing functions from the ISO 2631-1 [4]:

- Vertical accelerations of the individual point masses i.e. at users' seats
- The pitch and roll accelerations of the entire bus were projected to the users' location and this value was added or subtracted from the overall bus vertical acceleration to evaluate the vertical accelerations at the users' feet i.e. at the bus floor.
- The lateral accelerations were assessed at the users' seating location, backrest and feet by applying the relevant weighing factors mentioned in the ISO 2631-1 [4].

The roll and pitch accelerations considered for the bus users were equal to the roll and pitch acceleration of the sprung mass. Individual roll or pitch acceleration calculation for the individual point masses were not necessary due to the following assumptions:

- The vertical distance of the point masses coincides with the height of the centre of gravity and hence the acceleration experienced would be the same.
- The point masses are assumed to move only in the vertical direction and have no relative motion in the roll or pitch direction of the bus.

3.4.1 Evaluation of comfort

To assess the comfort of the users, accelerations on the backrest, seat surface and feet location in 6 DOF are considered. The lateral, roll, pitch and yaw acceleration are assumed to be the same at all body part locations. The vertical acceleration differs on the feet compared to the seat surface and backrest due to the seat suspension, which only acts in the vertical plane. 6 Different weighing filters were used for the different axes to obtain the weighted accelerations. The weighted accelerations signified the accelerations perceived by the human body in that particular direction.

From the obtained vertical and lateral accelerations at the user seating and floor, the Power Spectral Density (PSD) value was calculated based on the frequencies of the respective accelerations. PSD was preferred for evaluating the effect of accelerations on comfort levels since it takes into account the variation in accelerations in different frequency ranges. Therefore, it helped to point out the accelerations at frequencies that had a more profound effect on user comfort.

The weighted accelerations were also objectively assessed by using the comfort limits mentioned in chapter 2.1. For this assessment the total RMS value for all accelerations was calculated by using equation 1 in the same chapter.

Further, RMS values for each acceleration were also computed for comparisons and understanding of what factors affected the comfort.

3.4.2 Evaluation of motion sickness

The evaluation of motion sickness was objectively made with the formula for MSDV_z in equation 3 from chapter 2.1.1. Compared to the evaluation of ride comfort, there were no specified limits to compare the results with. The retrieved values were regarded as "the higher the MSDV_z, the higher the probability of becoming motion sick".

It must be noted that motion sickness is a highly subjective illness and that the MSDV_z only regards motion sickness due to vertical accelerations. No visuals or sounds were regarded in the motion sickness assessment, even though they probably are very important factors for motion sickness.

3.5 Caster implementation

To further evaluate the comfort of the bus, the driving simulator Cruden could be used. It is a driving simulator with 6 degrees of freedom located at Chalmers University of Technology.

The test could involve letting volunteers ride through the simulation, and make them answer questions on how they feel, if it was uncomfortable and if they felt motion sickness. A "blind test" is proposed, in the sense that the test objects should not know which seat they are testing.

3.5.1 Assumptions and constraints

Since the simulator does not have individual motion hydraulics for the seat compared to the floor, the only accelerations the test subject experienced were the seat's accelerations. The only difference between the seat's accelerations and the floor's accelerations is in the vertical plane. In the evaluation for motion sickness, the only acceleration with impact (according to the MSDV_z equation from ISO 2361-1 [4]) is vertical motion in the seat.

4 Results

The results of the simulation are presented in this chapter. Where the graphs and results are based on the 13 DOF bus model made in Matlab and Simulink. Ride comfort and motion sickness are evaluated and interpreted according to ISO 2631-1.

4.1 Simulation results for comfort

To analyse the results from the simulations, the vertical acceleration was plotted against time for each position on the bus. Figure 16 to Figure 19 show these graphs for the different bus velocities.

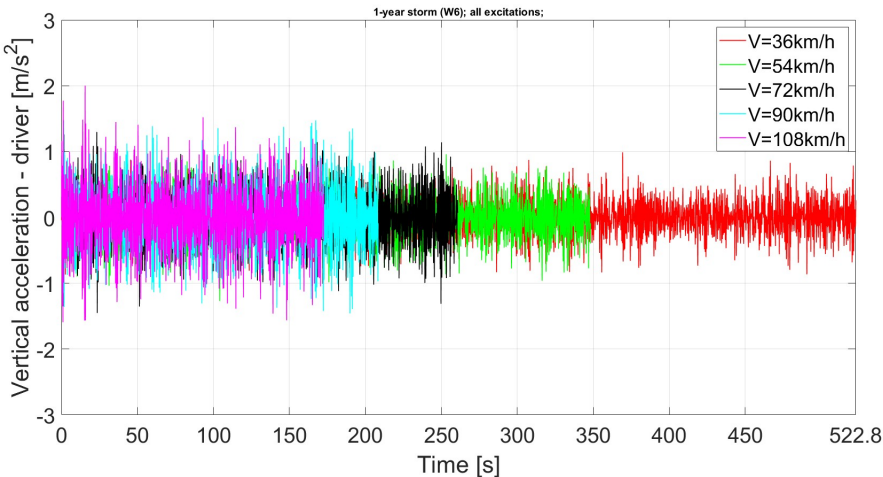


Figure 16: Resulting vertical acceleration at driver's seating position.

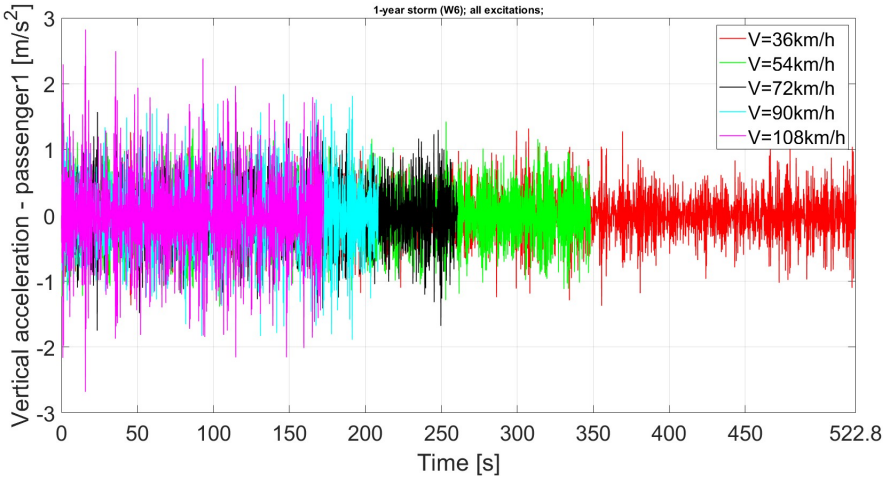


Figure 17: Resulting vertical acceleration at passenger 1 seating position.

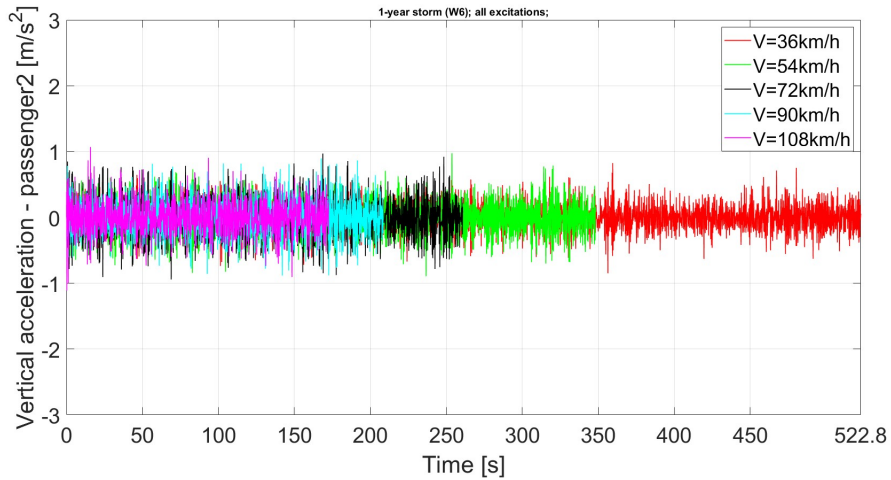


Figure 18: Resulting vertical acceleration at passenger 2 seating position.

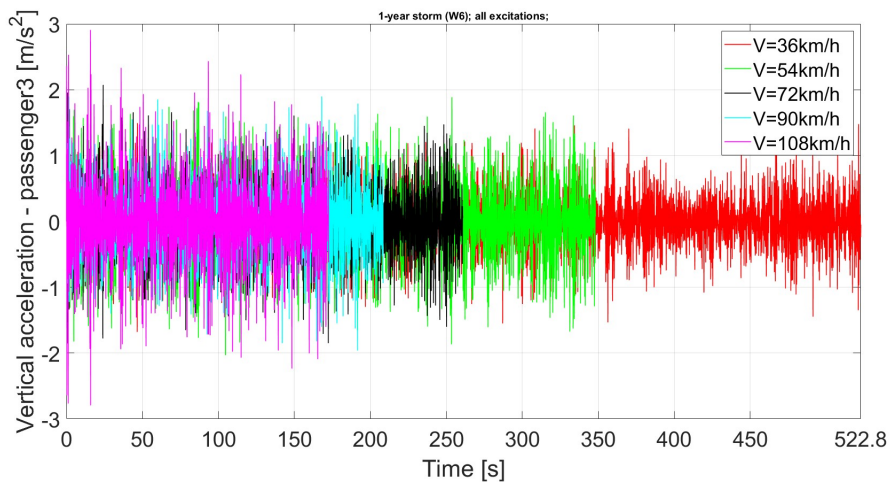


Figure 19: Resulting vertical acceleration at passenger 3 seating position.

The spread of vertical acceleration increases with the increased speed of the bus. The results also show that the seating locations furthest away from the COG experienced a higher level of vertical acceleration (Figure 16 - Driver and Figure 19 - Passenger 3). The seating locations closer to the COG experienced lesser excitation in vertical acceleration (Figure 18 - Passenger 2). The driver and passenger 1 were both placed at the bus front part (front overhang) at almost the same length from COG, but the driver experienced a lot less vertical acceleration due to their improved seat compared to the passengers' seat.

Figure 20 and figure 21 show the PSD of seat vertical acceleration for all users. Figure 20 shows the individual users seat dependent on the speed, and figure 21 shows all the users in

the same graph, but only for the speed 36 *km/h*.

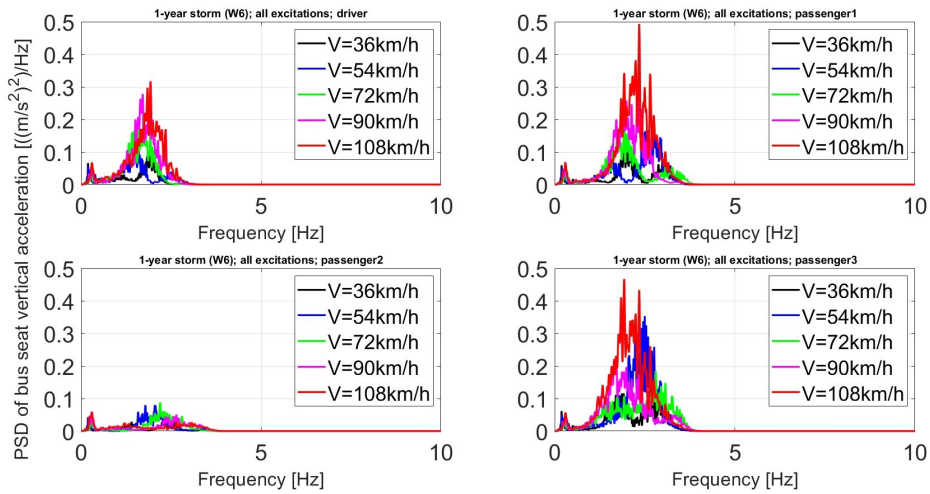


Figure 20: PSD of vertical accelerations at users' seats.

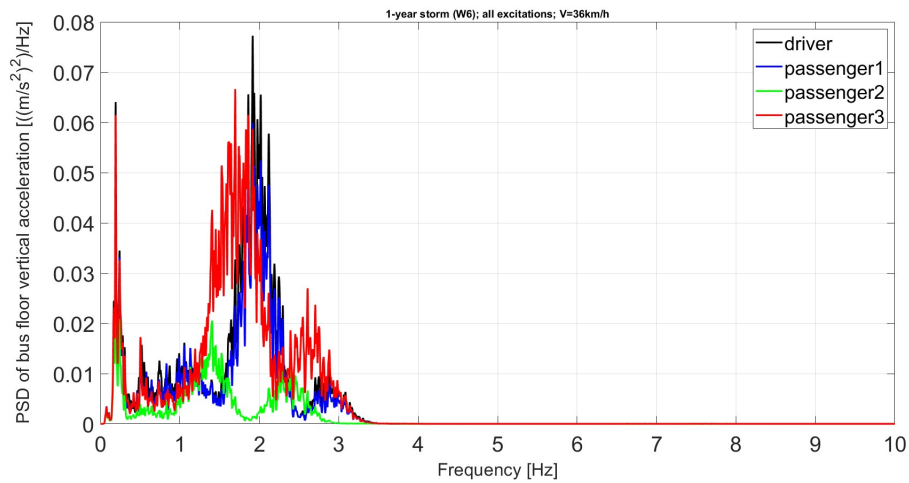


Figure 21: PSD of acceleration of bus floor at the user seating location.

The results show the most common frequencies of the accelerations to be between 2.5-3 Hz, they depend on the speed, with increasing frequency for higher speeds. The amplitude is highly dependent on both the speed and the seating position, increasing with further distance to COG

The next 2 graphs (figure 22 and 23) show the PSD of the bridge's lateral and vertical acceleration respectively for all tested speeds.

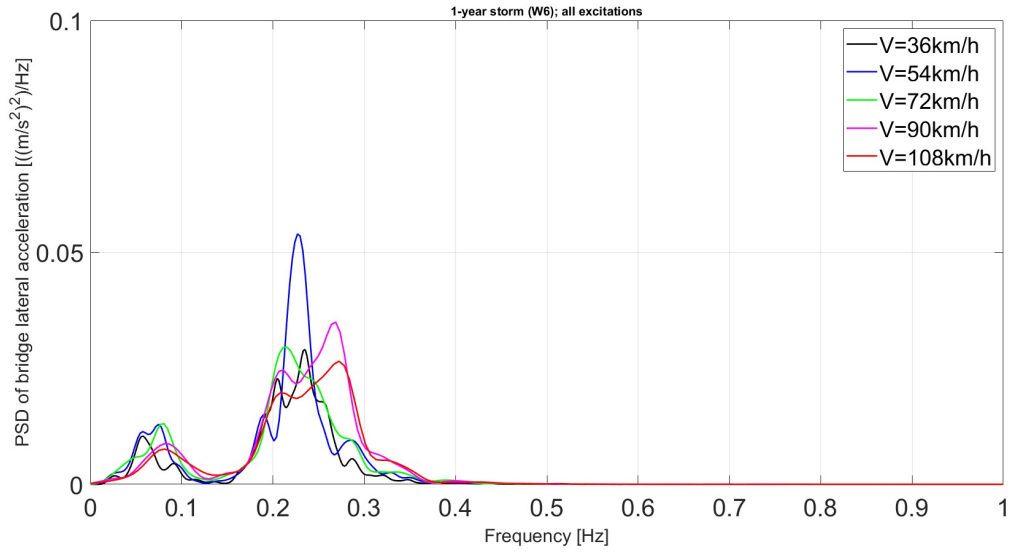


Figure 22: PSD of bridge lateral acceleration.

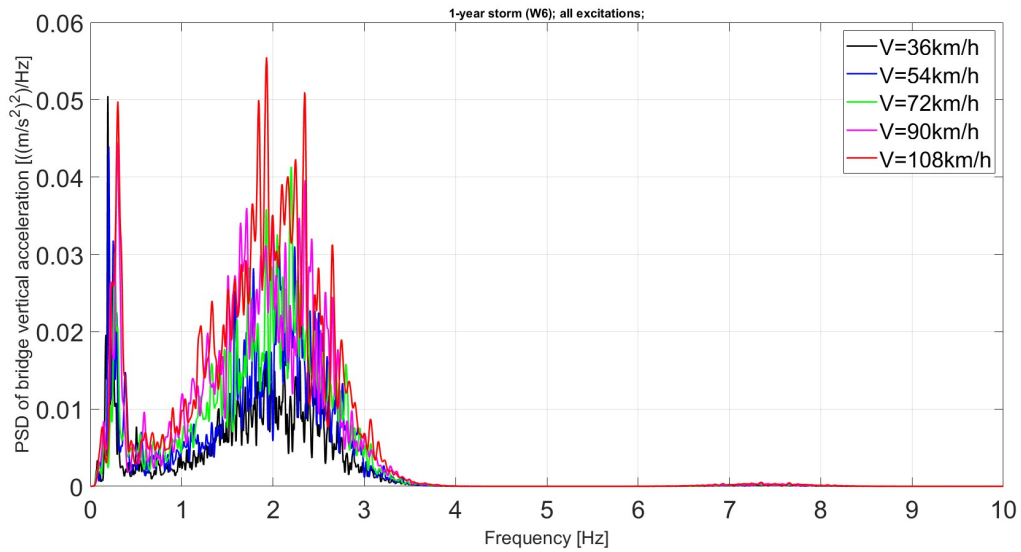


Figure 23: PSD of bridge vertical acceleration.

The vertical acceleration of the bridge corresponds roughly to the vertical accelerations of the bus COG seen in figure 24.

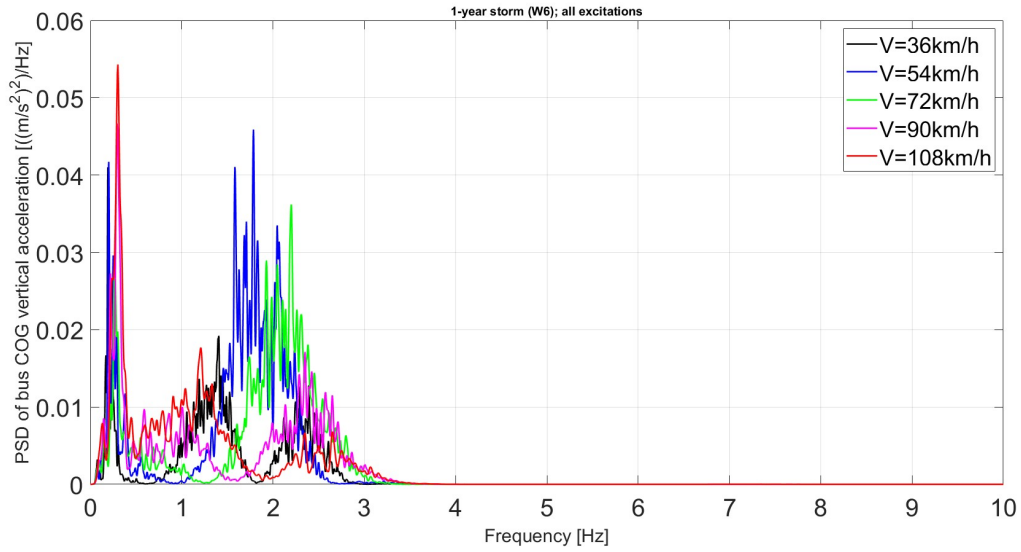


Figure 24: PSD of bus CoG vertical acceleration.

It can in figure 25 be seen that the bridge and the bus' COG vertical displacements are similar to each other. In some time domains, it can be seen that the bus is gaining some of the movement from the bridge. On other regions of the bridge, the bus displacements attenuate compared to the bridge movement.

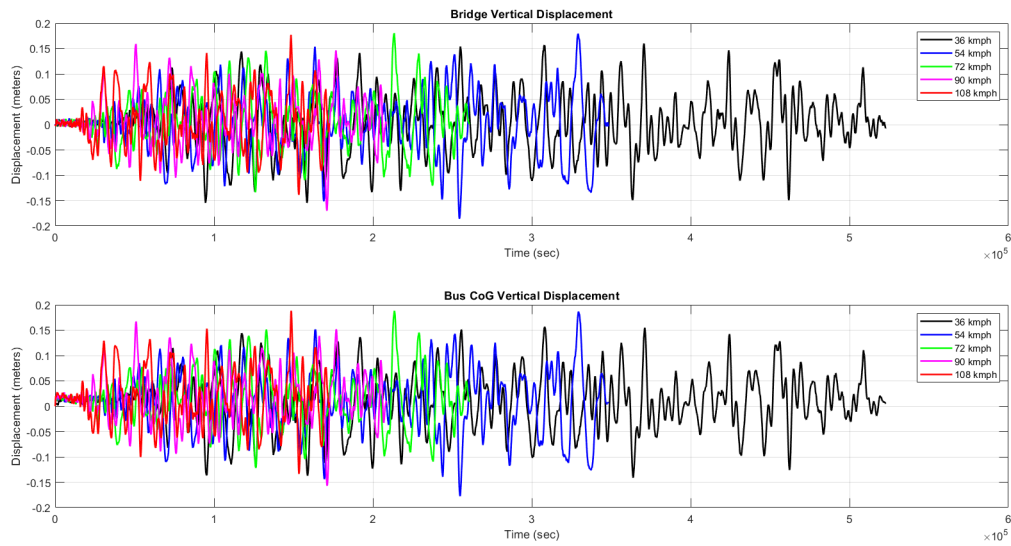


Figure 25: Vertical displacements of bridge and bus COG.

The following figures 26 to 29 show the RMS values of the weighted accelerations at the

users' seating position in the lateral and vertical directions with and without wind forces acting on the bus.

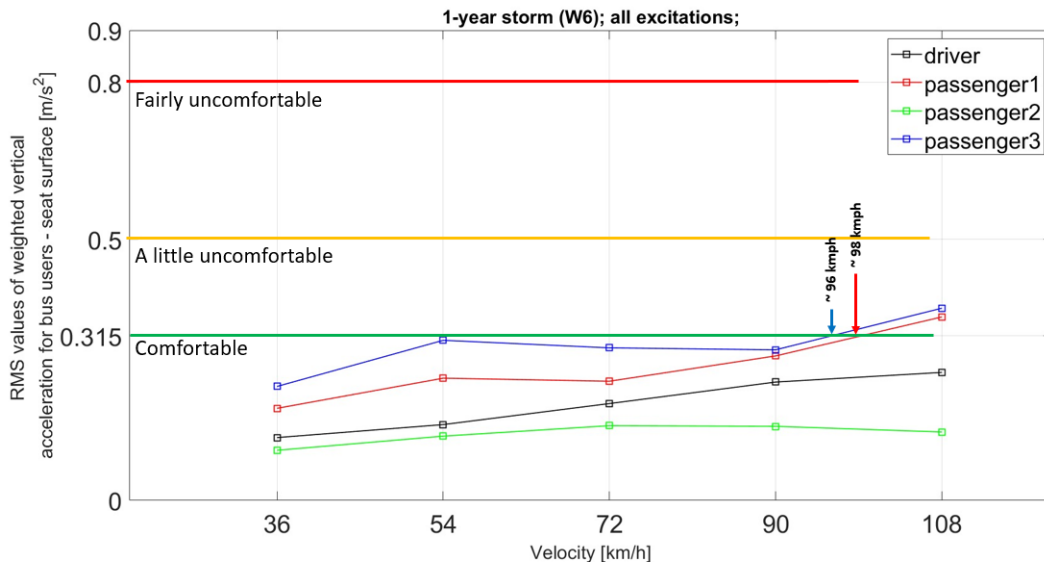


Figure 26: RMS value of the vertical acceleration at the users' seating location - with wind forces acting on the bus.

In figure 26 it is shown that the weighted vertical acceleration barely increases with speed, at least for speeds above 36 km/h but it is highly dependent on the user's seat placement.

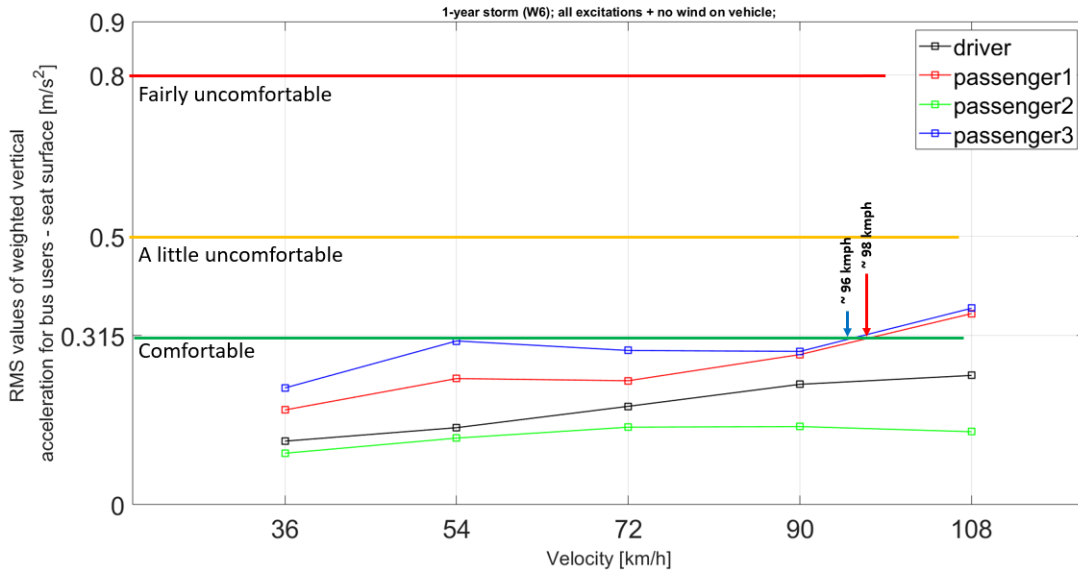


Figure 27: RMS value of the vertical acceleration at the users' seating location - without wind forces acting on the bus.

Figure 27 shows the weighted vertical acceleration without wind forces and moments acting on the bus. When compared to figure 26, it is clear that the vertical accelerations do not change due to the wind, as the wind only affects the bus laterally and makes it roll a bit. If the bus rolls a bit it can induce a heaving motion on the seats, resulting in a small vertical acceleration, but it can't be seen here since it's too small.

In the figures 28 and 29 we can see how the lateral acceleration of the vehicle is affected by the wind acting on the vehicle. In figure 28 when the wind is acting on the vehicle, the value of lateral accelerations experienced is higher and increases with respect to the vehicle velocity. Whereas in the case where no wind is acting on the vehicle, the lateral accelerations experienced are almost nil and remain constant irrespective of the vehicle velocity, as seen in figure 29.

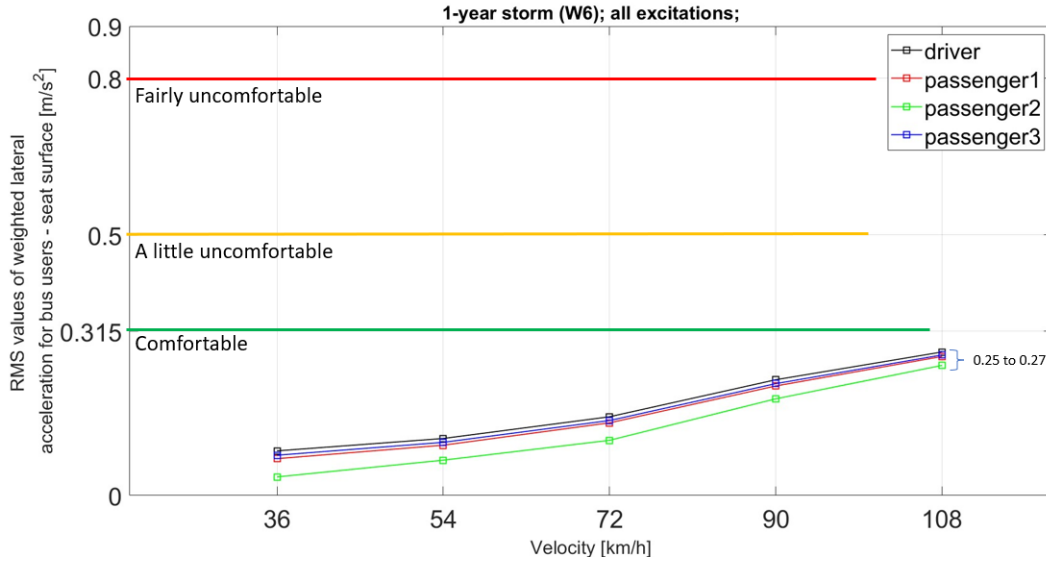


Figure 28: RMS value of total lateral acceleration at the users, seating location - with wind forces acting on the bus.

The weighted lateral acceleration increases with speed almost linearly and is barely dependent on seat placement compared to the vertical acceleration which is the other way around.

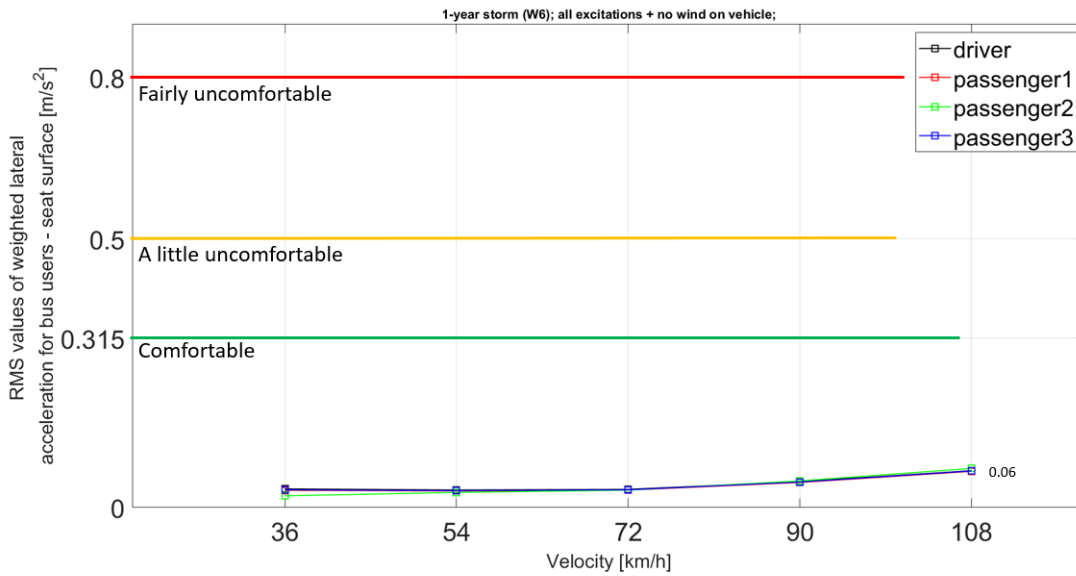


Figure 29: RMS value of total lateral acceleration at the users, seating location - without wind

When the wind is removed the lateral forces are almost negligible, the only affecting force to give any lateral acceleration is the steering of the bus to follow the road as it is slightly

curved sideways due to the wind and waves still acting on the bridge.

By adding all of the RMS values together from each direction (vertical, lateral, roll, pitch and yaw) the total RMS value can be calculated, as seen in figure 30. This is what the users would finally feel when travelling over the bridge on the bus. The passenger in the front and the rear starts feeling fairly uncomfortable at speeds above 100 km/h, and even passenger 2, located in the middle of the bus, starts feeling a little uncomfortable.

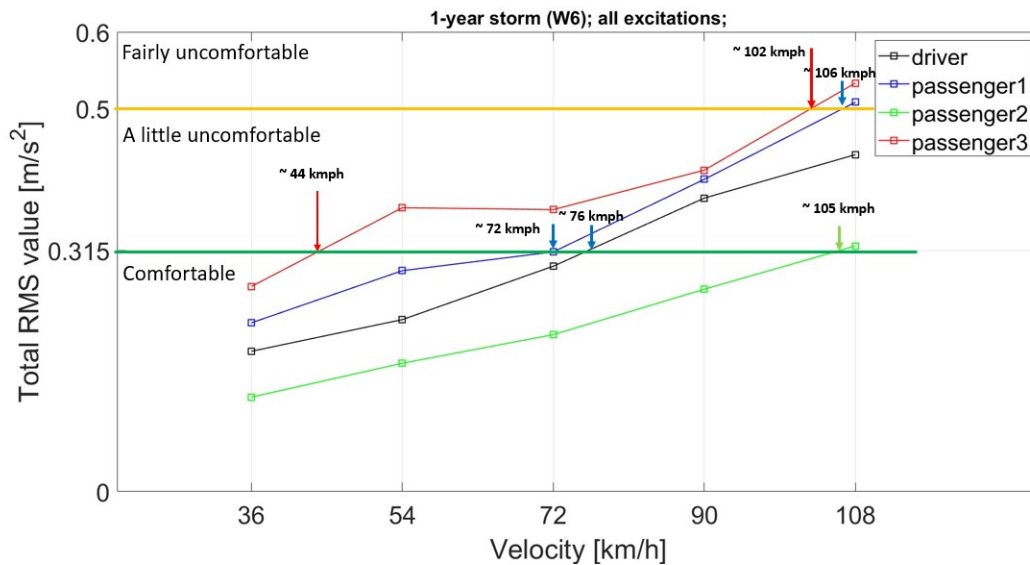


Figure 30: RMS value of the total accelerations.

The same is done for the simulation without wind. The big difference, as seen before, is the reduced lateral accelerations, reducing the total RMS value. (Figure 31)

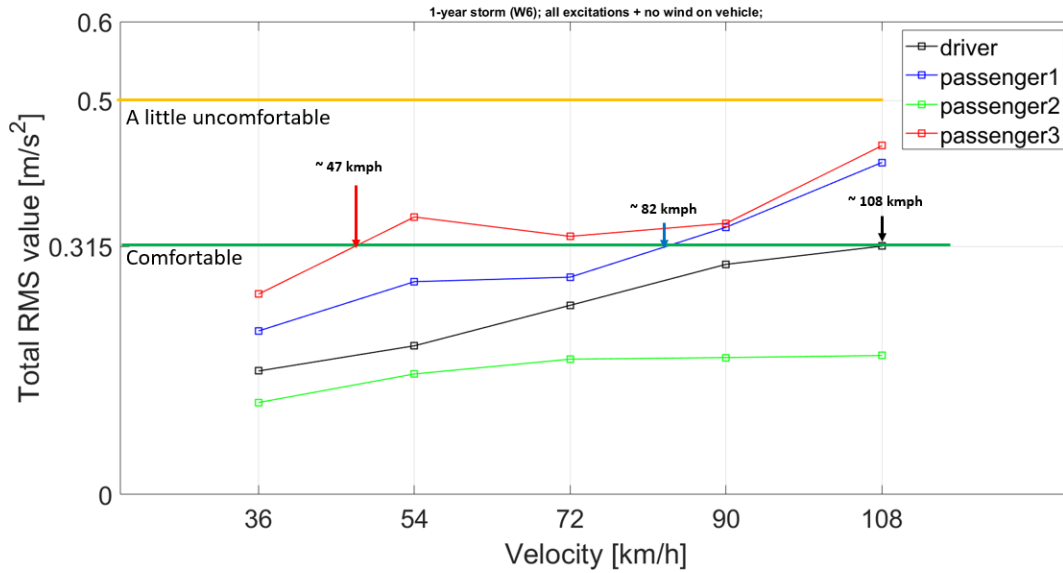


Figure 31: RMS value of the total accelerations - no wind forces acting on the bus.

Figure 32 shows the total RMS value for the 2-year storm condition. It can be seen that all the passengers become "a little uncomfortable" at slower speeds than for a 1-year-storm condition. No simulation results were retrieved for 108 km/h in the 2-year-storm condition because it's known from [8] that the bus isn't laterally stable for that velocity.

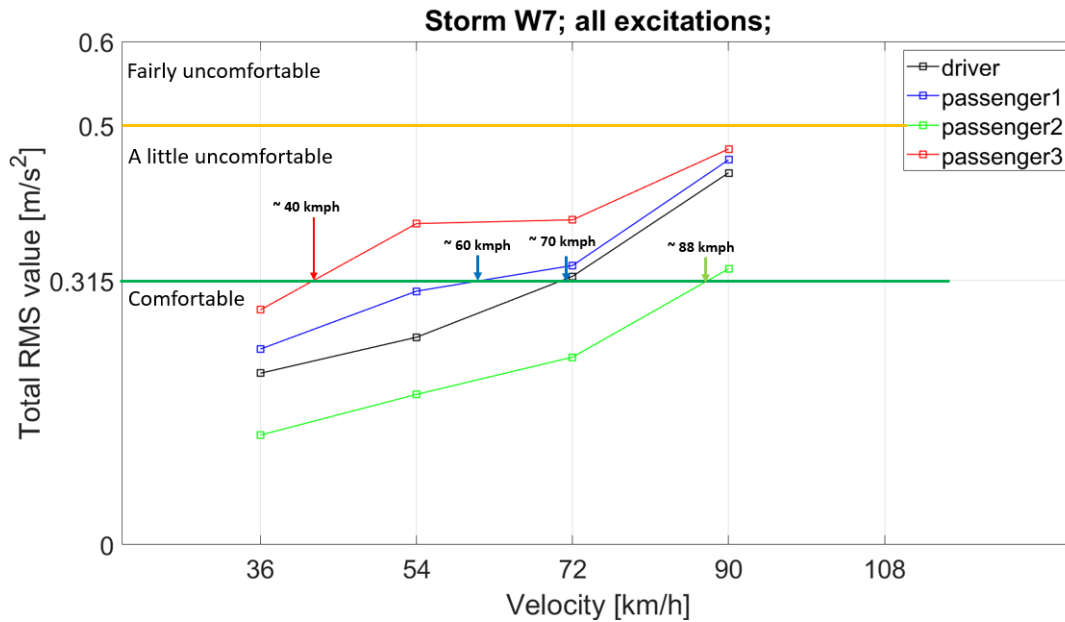


Figure 32: RMS value of the total accelerations - 2-year storm condition.

As can be seen from the graphs, the seating position of the user has a more profound impact on the experienced vertical accelerations while the perceived lateral acceleration has a very minimal deviation from the positioning.

4.2 Simulation results for motion sickness

Figure 33 shows the PSD for each passenger’s weighted vertical accelerations for motion sickness assessment. Accelerations regarding motion sickness are mainly felt in the frequencies of 0.15-0.3 Hz, with a significant peak at approximately 0.2 Hz. The magnitudes of the accelerations are similar for the users that are seated far away from the COG of the bus. Passenger 2 who is seated closer to the COG of the bus experiences less acceleration concerning motion sickness.

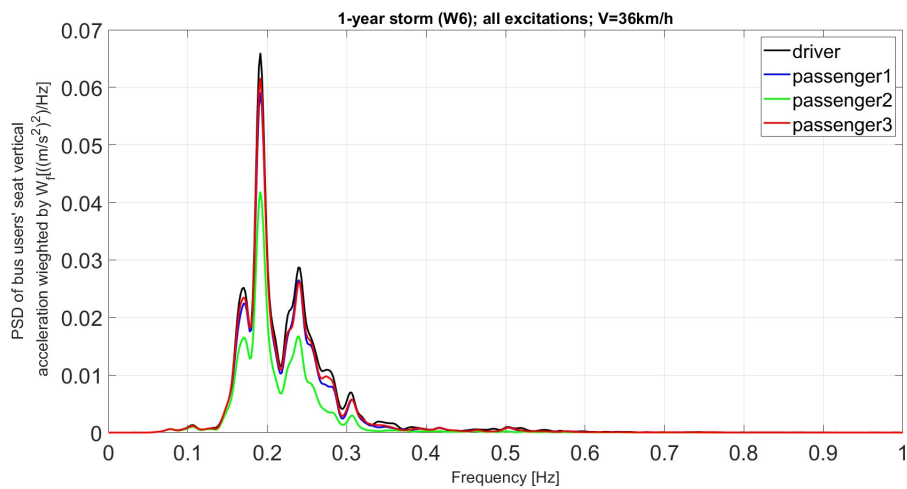


Figure 33: PSD for weighted vertical acceleration at the seat for motion sickness evaluation.

The MSDVz for different speeds for each passenger are seen in figures 34 and 35. The first one is with wind acting on the bus and the second one is without wind acting on the bus.

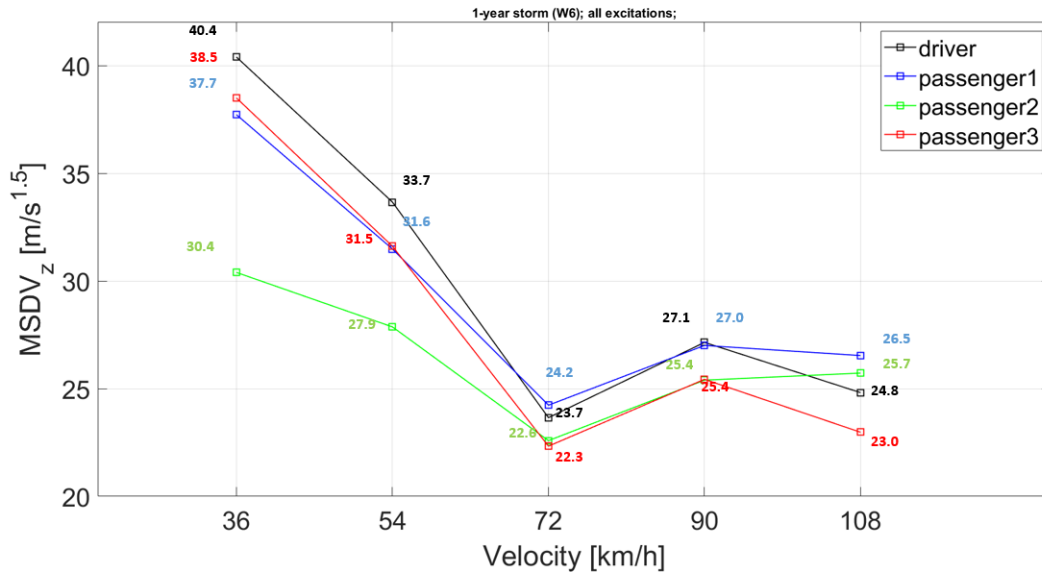


Figure 34: MSDV_z for different speeds - with wind forces acting on the bus.

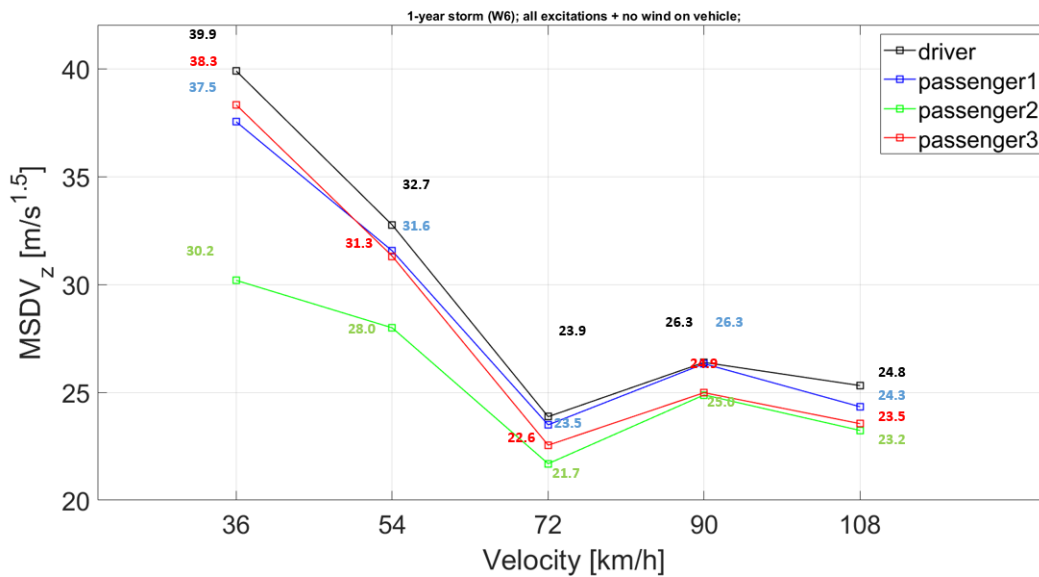


Figure 35: MSDV_z for different speeds - without wind forces acting on the bus.

For both cases, the highest MSDV_z are found in the slowest speed. This can be explained by the time it takes for the slower-moving bus to drive over the bridge, and the dose value depends on the total time experiencing the accelerations.

Figure 36 below show the MSDV_z results for the 2-year-storm condition. The same velocity trend remains, but all values have increased slightly.

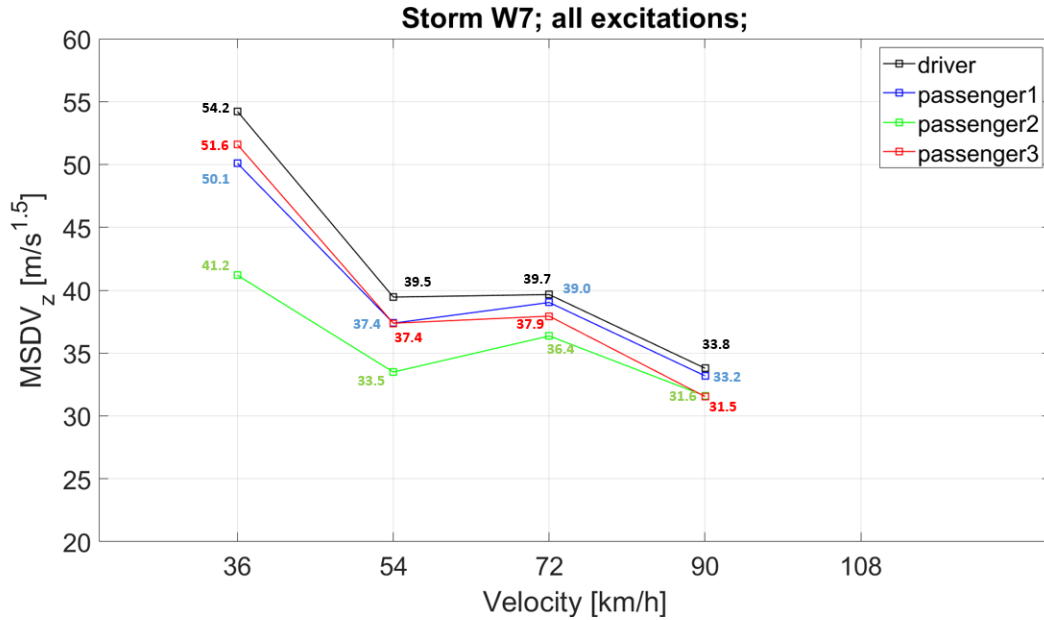


Figure 36: MSDVz for different speeds - 2-year storm.

From these MSDVz results it can be observed that the probability of getting motion sick is higher at speeds between 36 and 72 km/h compared to speeds higher than 72 km/h.

4.3 Caster implementation

To be able to implement the Cruden simulator as an assessment tool, several assignments had to be done. Some of these were easier to fix than others. What was managed in the Caster implementation was the correct Simulink model, receiving filtered acceleration and the creation of the header and dat file.

The first problem that occurred was the amplitudes of some of the accelerations and thereby the translation going out of bounds on the simulator. To compensate for this phenomenon, a high pass filter needed to be applied to all of the accelerations and translations that went out of bounds.

After the translation amplitudes were checked to be in bounds, 2 files were created for the simulator to be able to read the data. To create these files, help was needed directly from Cruden, providing a Matlab-script that read the data files and created the 2 new files needed, a header file and a dat file.

To run these, the simulator itself needed to be updated to a newer version of the software. The update itself was fairly easy to perform, but with little to none experience with the newer version of the software, the simulation was not able to be done before the deadline of the project.

5 Discussion

This project involved simulations of different driving conditions in different velocities with four contrasting seating positions. To be able to perform trustworthy simulations, a bus model with 13 DOF, instead of 8 DOF from [2], was used. What differed in this project, from the previously mentioned papers, was that the bus model also included motions for one driver, three passengers and pitch motion.

The bus occupants consisted of one driver, who sat in front of the front axle, one passenger above the same axle, one passenger close to the COG and the third passenger above the rear axle. The compared results between the mentioned occupants were interesting, hence the actual variation in results of the ride comfort and motion sickness.

5.1 Discussion of ride comfort results

According to the standard ISO 2631-1 and the weighting filters the ride comfort is mainly assessed in the frequency interval $0.5 - 80 \text{ Hz}$. The limits used for assessment of the ride comfort can also be found in ISO 2631-1, which can be seen as objective limits for the evaluation. The magnitudes, the frequencies and the amount of time during these conditions of the accelerations affecting human health are not considered. Therefore, this evaluation method cannot be used for long-term exposure to vibrations.

It could be seen that the key factor affecting the ride comfort is vertical acceleration which is highly affected by the seat position on the bus. The lateral accelerations also had a big impact due to the wind. The seating position barely affected the lateral, roll, pitch and yaw accelerations. But the influence of speed is a crucial element to the ride comfort. Worth mentioning, is that the driver model has an impact on the ride comfort, hence the steering inputs to compensate for the wind acting on the bus.

It was seen that when seated closest to the COG the ride comfort was better. It could also be seen that the bus driver had a more comfortable bus ride over the floating bridge compared to passenger 1. They had similar seat positions but experienced different ride comfort, hence the driver had an improved seat suspension compared to the passengers who were seated on regular cushioned seats.

5.2 Discussion of motion sickness results

Since motion sickness is a highly subjective feeling, the results were only compared between the different weather conditions and for different velocities. Motion sickness is also affected by where the bus occupant is seated. The experienced motion sickness is dependent on hearing, where the passenger is looking and the air quality in the bus [9]. The level of motion sickness also depends on gender and age, where females and younger persons are more prone to it [4]. With this in mind, the MSDVz for the vertical displacement is a, for

this project, sufficient way of rating the different driving scenarios objectively, but it still has to be taken into account that motion sickness is a highly subjective illness.

It was seen in the weighting factor that the motion sickness dose value was evaluated in the lower frequency interval. The wave energy causes the typical low-frequency swaying motion that contributes to motion sickness [10]. This is caused by the wave energy and could also be seen in the graphs over the PSD.

It could also be noticed that the 1- and 2-year storm conditions do not have a huge impact on motion sickness. The conclusion from this is that the magnitude of the bridge excitation has a marginal impact on the MSDVz, while the time has a highly strong impact. Comparing the different traveling speeds the motion sickness level where noticeably higher for the lower speeds, due to the longer travel time over the bridge. The total time of riding over the floating bridge is between 3 and 10 minutes which is probably an unusually short duration for motion sickness assessment. According to the ISO standard 2631-1 [4], these relationships are based on motions where the person experiences motion sickness for at least 20 minutes to 6 hours.

5.3 Future work

5.3.1 Testing more storm conditions

To further evaluate the comfort of the bus in different weather conditions, more storm conditions could be tested, both rare and intense storms, as well as more regular easier ones to see the impact.

5.3.2 Caster implementation and blind test

Unfortunately, the tests in Caster were not ready in time, which meant no results from the Caster implementation. The time-plan for the Caster implementation took longer than expected due to a few reasons mentioned in 4.3.

To evaluate how different comfort levels and MSDVz feel subjective, a blind test could be done by letting test subjects test different storm conditions and speeds, and then evaluate their comfort level and compare it against the ISO 2361-1 standard limits for comfort.

5.3.3 Varying bus parameters

To further investigate the comfort of a bus driving on the bridge, the vehicle parameters could be varied to see how the comfort is affected. This could be done by only changing one or a few parameters, for example, the suspension to see how the bus reacts.

Another approach could be to implement a known vehicle's parameter to test that certain vehicle.

6 Notations

Bus Parameter	Units	Notation	Value
Mass of Driver	kg	m_d	80
Mass of Passenger 01	kg	m_1	80
Mass of Passenger 02	kg	m_2	80
Mass of Passenger 03	kg	m_3	80
Sprung Mass	kg	m_s	16099
Front Un-Sprung Mass	kg	m_{uf}	746
Rear Un-Sprung Mass	kg	m_{ur}	1355
Sprung mass moment of inertia X-Axis	kgm^2	J_{sx}	33400
Sprung mass moment of inertia Y-Axis	kgm^2	J_{sy}	150000
Sprung mass moment of inertia Z-Axis	kgm^2	J_{sz}	290000
Front un-sprung mass moment of inertia X_f Axis	kgm^2	J_{ufx}	315
Rear un-sprung mass moment of inertia X_r Axis	kgm^2	J_{urx}	657
Wheel Base	m	L	8.3750
Distance from front axle to COG	m	l_f	4.4103
Distance from rear axle to COG	m	l_r	3.9647
Track width front axle	m	tw_f	2.00
Track width rear axle	m	tw_r	2.00
Total bus COG height	m	h_{CoG}	1.1725
Front axle roll center height (Axle COG)	m	h_{RCf}	0.508
Rear axle roll center height (Axle COG)	m	h_{RCr}	0.508
Distance in Z-Axis from front axle roll center to COG	m	$h_{RCf2CoG}$	0.6645
Distance in Z-Axis from rear axle roll center to COG	m	$h_{RCr2CoG}$	0.6645
Distance in Z-Axis from COG to roll axis	m	Δh_{RC2CoG}	0.6645
Dist. in Y-Axis from front suspension element to COG of front axle	m	e_{uf}	0.70
Dist. in Y-Axis from rear suspension element to COG of rear axle	m	e_{ur}	0.80
Single shock absorber damping on rear axle	Ns/m	c_r	22500
Single spring (air bag) stiffness on rear axle	N/m	k_r	200000
Single shock absorber damping on front axle	Ns/m	c_f	20000
Single spring (air bag) stiffness on front axle	N/m	k_f	175000
Single rear tyre stiffness	N/m	k_{tr}	2000000
Combined rear tyre stiffness	N/m	$k_{tot,tr}$	4000000

Bus Parameter	Units	Notation	Value
Single front tyre stiffness	N/m	k_{tf}	1000000
Combined front tyre stiffness	N/m	$k_{tot,tf}$	2000000
Front anti roll bar stiffness	Nm/rad	$k_{arb,f}$	120000
Rear anti roll bar stiffness	Nm/rad	$k_{arb,r}$	120000
Front axle roll stiffness due to corner springs	Nm/rad	$k_{\phi,f}$	343000
Rear axle roll stiffness due to corner springs	Nm/rad	$k_{\phi,r}$	512000
Front axle roll damping due to corner dampers	Nms/rad	$c_{\phi,f}$	39200
Rear axle roll damping due to corner dampers	Nms/rad	$c_{\phi,r}$	57600
Displacement of sprung mass	m	z_s	Simulated
Displacement of front unsprung mass	m	z_{uf}	Simulated
Displacement of rear unsprung mass	m	z_{ur}	Simulated
Displacement of driver seat	m	z_d	Simulated
Displacement of passenger 01 seat	m	z_{p1}	Simulated
Displacement of passenger 02 seat	m	z_{p2}	Simulated
Displacement of passenger 03 seat	m	z_{p3}	Simulated
Roll angle of sprung mass	rad	ϕ_s	Simulated
Roll angle of front unsprung mass	rad	ϕ_{uf}	Simulated
Roll angle of rear unsprung mass	rad	ϕ_{ur}	Simulated
Pitch angle of sprung mass	rad	θ_s	Simulated
Yaw rate of sprung mass	rad/s	ω_z	Simulated
Distance from COG to driver along Y-Axis	m	s_1	0.65
Distance from COG to driver along X-Axis	m	s_2	5.91
Distance from COG to passenger 1 along Y-Axis	m	s_3	0.8
Distance from COG to passenger 1 along X-Axis	m	s_4	5.2103
Distance from COG to passenger 2 along Y-Axis	m	s_5	0.8
Distance from COG to passenger 2 along X-Axis	m	s_6	0.5
Distance from COG to passenger 3 along Y-Axis	m	s_7	0.4
Distance from COG to passenger 3 along X-Axis	m	s_8	5.4647
Distance from COG to passenger 3 along X-Axis	m	s_8	5.4647
Distance from COG to passenger 3 along X-Axis	m	s_8	5.4647
Road roughness value of front right contact patch	m	ξ_{fr}	Simulated
Road roughness value of front left contact patch	m	ξ_{fl}	Simulated
Road roughness value of rear right contact patch	m	ξ_{rr}	Simulated
Road roughness value of rear left contact patch	m	ξ_{rl}	Simulated
Steering angle	rad	δ	Simulated
Frontal area of the bus	m^2	A	8.23
Aerodynamic drag coefficient	-	C_d	function of β_w
Aerodynamic side coefficient	-	C_s	function of β_w
Aerodynamic lift coefficient	-	C_l	function of β_w
Aerodynamic roll coefficient	-	C_R	function of β_w
Aerodynamic pitch coefficient	-	C_P	function of β_w
Aerodynamic yaw coefficient	-	C_Y	function of β_w

Weighting multiplying factor	Units	Notation	Value
Multiplying factor - floor - Vertical	-	$k_{z, floor}$	0.40
Multiplying factor - floor - Lateral	-	$k_{y, floor}$	0.25
Multiplying factor - Backrest - Vertical	-	$k_{z, seat-back}$	0.40
Multiplying factor - Backrest - Lateral	-	$k_{y, seat-back}$	0.50
Multiplying factor - Seat - Vertical	-	$k_{z, seat}$	1.0
Multiplying factor - Seat - Lateral	-	$k_{y, seat}$	1.0
Multiplying factor - Seat - Roll	m/rad	$k_{roll, seat}$	0.63
Multiplying factor - Seat - Pitch	m/rad	$k_{pitch, seat}$	0.40

Sources

- [1] COWI, “The world’s longest floating bridge over Bjørnafjord.” [Online]. Available: <https://www.cowi.com/solutions/infrastructure/bjoernafjord-ground-breaking-floating-bridge-for-a-ferry-free-e39-norway> [Accessed: 21/12/2023]
- [2] D. Sekulić, V. Dedović, S. Rusov, S. Šalinić, A. Obradović, “Analysis of vibration effects on the comfort of intercity bus users by oscillatory model with ten degrees of freedom,” *Applied Mathematical Modelling*, 2013.
- [3] D. Sekulić, A. Vdovin, B. Jacobson, S. Sebben, S. M. Johannesen, “Effects of wind loads and floating bridge motion on intercity bus lateral stability,” *Journal of Wind Engineering & Industrial Aerodynamics*, 2021.
- [4] ISO – International Organization for Standardization, “ISO 2631: Mechanical vibration and shock-evaluation of human exposure to whole-body vibration, second ed.” 1997. [Online]. Available: <https://www.sis.se/produkter/miljo-och-halsoskydd-sakerhet/vibration-med-avseende-pa-manniskor/ssiso26311/> [Accessed: 13/10/2023]
- [5] B. J. et al, “*Compendium in Vehicle Motion Engineering*”. Vehicle Dynamics Group, Division Vehicle and Autonomous Systems, Department of Mechanics and Maritime Sciences, Chalmers University of Technology, 2023.
- [6] “Cruden B.V. — Automotive driving simulators,” 2023. [Online]. Available: <https://www.cruden.com/automotive-driving-simulators/> [Accessed: 5/1/2024]
- [7] “Caster Chalmers — Student community,” 2023. [Online]. Available: <https://www.casterchalmers.se/> [Accessed: 5/1/2024]
- [8] Sekulic, D., Vdovin, A., Jacobson, B., Sebben, S., Johannesen, S, “Determination of safe speeds for a coach travelling on a floating bridge,” *Transportation Research Interdisciplinary Perspectives (Submitted)*, 2023.
- [9] Leung AK, Hon KL, “Motion sickness: an overview,” *Drugs Context*, 2019.
- [10] Ryan G. Coe, Giorgio Bacelli, Dominic Forbush, “A practical approach to wave energy modeling and control,” *Renewable and Sustainable Energy Reviews*, 2021.